Seasonal Migration, Gene Flow, and Speciation in North American Birds

C. J. Battey

A dissertation
submitted in partial fulfillment of the
requirements for the degree of

Doctor of Philosophy

University of Washington
2018

Reading Committee:

John Klicka, Chair
Adam Leaché
Lauren Buckley

Program authorized to offer degree:
Biology

University of Washington

Abstract

Seasonal Migration, Gene Flow, and Speciation in North American Birds

C. J. Battey

Chair of Supervisory Committee: John Klicka
Department of Biology

Around 20% of bird species migrate annually between distinct breeding and wintering ranges[1], and many sedentary populations shift cyclically within a single range in response to varying climates and food availability. Migration allows populations to take advantage of seasonal resource abundance and access isolated habitat patches, but it comes with significant costs. Individuals have to build up large fat reserves to power the journey, and must navigate huge distances in their first year of life. At a population level, migratory species experience high levels of gene flow between distant areas of the breeding range, which maintains genetic diversity but makes local adaptation difficult because of a continuous inflow of alleles from off-target migrants. Conversely, when migratory behaviors are themselves heritable they can reinforce population differentiation by selecting against unfit hybrids. However, we know relatively little about migratory connectivity or genetic diversity across the range in most species, and it is unclear if the few examples of migratory variation associated with genetic differentiation are the exception or the rule. Is seasonal migration a homogenizing force during speciation, or a differentiating one?

In this dissertation I study three examples of migratory birds in the early stages of speciation, and ask how migratory patterns shape genetic diversity during lineage divergence. In chapter 1, I test for gene flow and estimate species limits in the Red-Eyed Vireo (*Vireo olivaceus*) species complex – a group of four to seven species that breed in disjunct habitats around the Americas and winter in sympatry in northern South America. Next I use a combination of breeding and wintering range samples from the Painted Bunting (*Passerina ciris*) to map migratory connectivity in the species, and identify an unexpected link between breeding populations in the lower Mississippi River Valley and wintering populations on the Yucatán Peninsula. Last, I sequence and analyze the complete genomes of the Rufous, Allen's, and Calliope Hummingbirds (*Selasphorus rufus, sasin* and *calliope*, respectively) in order to map geographic population structure and identify regions of the genome under disruptive selection across species.

[1]Kirby et al. (2008)

Contents

1 Cryptic Speciation and Gene Flow in a Migratory Songbird Species Complex: Insights from the Red-Eyed Vireo (*Vireo olivaceus*) 5

1.1 Abstract . . . 6
1.2 Introdution . . . 7
1.3 Methods . . . 8
1.3.1 Sampling and library preparation . . . 8
1.3.2 Sequence Assembly . . . 8
1.3.3 Phylogenetics . . . 9
1.3.4 Clustering and Ordination . . . 9
1.3.5 Admixture analysis . . . 9
1.3.6 Species delimitation with Bayes factors . . . 10
1.4 Results . . . 10
1.4.1 RAD loci and missing data . . . 10
1.4.2 Phylogenetics . . . 12
1.4.3 Clustering . . . 12
1.4.4 Admixture . . . 13
1.4.5 Coalescent species delimitation . . . 14
1.5 Discussion . . . 15
1.5.1 Migration, range, and gene flow . . . 15
1.5.2 Species delimitation . . . 16
1.5.3 Mito - nuclear discordance . . . 17
1.6 Conclusions . . . 17
1.7 Supplement and Data accessibility . . . 17
1.8 Supplementary Tables . . . 18
1.9 Acknowledgements . . . 19

2 A Migratory Divide in the Painted Bunting (*Passerina ciris*) 20

2.1 Abstract . . . 21
2.2 Introduction . . . 22
2.3 Methods . . . 23
2.3.1 Genetic Sampling . . . 23
2.3.2 Genotype Clustering and Population Assignment . . . 23
2.3.3 Mitochondrial DNA . . . 24
2.3.4 Demographic Modeling . . . 24
2.3.5 Morphology . . . 26
2.4 Results . . . 26
2.4.1 Sequence Assembly . . . 26

2.4.2 Genotype Clustering . . . 26
2.4.3 MtDNA . . . 27
2.4.4 Demographic Modeling . . . 27
2.4.5 Morphology . . . 29
2.5 Discussion . . . 30
2.5.1 Migratory Connectivity . . . 30
2.5.2 Phylogeography . . . 30
2.5.3 Implications for Conservation . . . 31
2.6 Conclusions . . . 31
2.7 Supplement and Data Availability . . . 32
2.8 Acknowledgements . . . 32

3 Evidence of Linked Selection on the Z Chromosome of Hybridizing Hummingbirds 36
3.1 Abstract . . . 37
3.2 Introduction . . . 38
3.2.1 Natural History of Northern *Selasphorus* Hummingbirds . . . 39
3.3 Methods . . . 39
3.3.1 Sampling . . . 39
3.3.2 Sequence Assembly . . . 40
3.3.3 Phylogenetics and Population clustering . . . 41
3.3.4 Demographic Models . . . 42
3.3.5 Introgression . . . 43
3.3.6 Genome Scans . . . 43
3.4 Results . . . 44
3.4.1 Phylogenetics and Population Structure . . . 44
3.4.2 Demography . . . 45
3.4.3 Introgression . . . 45
3.4.4 Genome Scans . . . 46
3.5 Discussion . . . 48
3.5.1 Phylogeography . . . 48
3.5.2 Migratory Connectivity in ***S. rufus*** . . . 49
3.5.3 Linked Selection and Sex Chromosome Differentiation . . . 50
3.5.4 Systematics . . . 50
3.6 Conclusion . . . 51
3.7 Data . . . 52
3.8 Acknowledgements . . . 52
3.9 Supplementary Figures and Tables . . . 53

Chapter 1

Cryptic Speciation and Gene Flow in a Migratory Songbird Species Complex: Insights from the Red-Eyed Vireo (*Vireo olivaceus*)

1.1 Abstract

Migratory species that alternate between sympatry and allopatry over the course of an annual cycle are promising subjects for studies seeking to understand the process of speciation in the absence of strict geographic isolation. Here we sought to identify cryptic species and assess rates of gene flow in a clade of neotropical migrant songbirds in which geography and taxonomy are currently out of sync: the Red-Eyed Vireo (*V. olivaceus*) Species Complex. Phylogenetic, clustering, and statistical species delimitation analyses found that *V. olivaceus* includes two non-sister lineages migrating in opposite directions across the equator. Analyses of gene flow identified low levels of introgression between two species pairs, but none between northern and southern *olivaceus*. We also identified substantial well-supported conflicts between nuclear and mitochondrial topologies. Although the geographic distribution of mito-nuclear discordance is suggestive of hybridization and mitochondrial capture, we found no evidence of introgression in the nuclear genome of populations with discordant mitochondrial gene trees. Our study finds that species boundaries match breeding range and migratory phenology rather than the existing taxonomy in this group, and demonstrates the utility of genomic data in inferring species boundaries in recently diverged clades.

*John Klicka was a coauthor on the published version of this chapter in *Molecular Phylogenetics and Evolution*: https://doi.org/10.1016/j.ympev.2017.056 .

1.2 Introdution

Geographic isolation is thought to be the dominant factor in initiating speciation in birds (Mayr, 1948; Mayr and O'Hara, 1986; Coyne and Price, 2000; Phillimore et al., 2008), and comparative studies often focus on the role of range gaps and geographic barriers in generating species diversity (Smith et al., 2014; Barber and Klicka, 2010; Zink et al., 2001). For migratory species, the role of allopatry in lineage divergence is unusual. Most individuals are physiologically capable of moving between disjunct ranges even when separated by large distances, but populations are isolated by heritable variation in the direction and timing of migration (Helbig, 1991; Pulido et al., 2001; Delmore and Irwin, 2014). In some cases sister species are allopatric during the breeding season and sym- or parapatric during the nonbreeding season, as occurs in many neotropical migrants breeding in northern temperate regions and wintering in Central and South America. Rates of gene flow across the ranges of these species are dependent on levels of migratory connectivity and distance of natal dispersal, rather than simple inertia in natal location.

The extensive spatial mixing associated with seasonal migration suggests that migratory species are promising subjects for studies seeking to better understand the role of gene flow in speciation. Recent studies in songbirds such as Redpolls (*Acanthis*) (Mason and Taylor, 2015), Greenish Warblers (*Phylloscopus trochiloides*) (Irwin et al., 2005), and Darwin's Finches (*Geospiza sp.*) (Lamichhaney et al., 2015) have found evidence of extensive introgression among morphologically divergent populations. In some cases (e.g. *Geospiza, Acanthis*) phenotypic plasticity and divergent selection on a small number of genes is thought to drive morphological variation despite a largely panmictic nuclear genome. One recent whole-genome sequencing study of hybridizing Golden- and Blue-winged warblers (*Vermivora chrysoptera* and *V. cyanoptera*, respectively), found that just 6 genomic regions appear to control phenotypic variation between species despite extensive introgression across the genome (Toews et al., 2016). These studies are part of an increasing focus on the extent and impacts of hybridization on speciation (and, in corollary, the biological meaning of taxonomic designations).

In this study we assess the consequences of divergent migratory behavior on speciation and gene flow in a systematically recalcitrant clade of neotropical songbirds: the Red-Eyed Vireo (*V. olivaceus*) Species Complex. This group includes three widespread migratory species that are sympatric in northern South America during the nonbreeding season and para- or allopatric during the breeding season. Unusually, the most widespread species in the group – *V. olivaceus* – includes populations migrating both north and south of the equator, as well as sedentary populations breeding in northern South America. Due to similar habits, vocalizations, and morphologies, earlier taxonomists typically recognized three (Mayr and Short, 1970) or four (Paynter, 1968; American Ornithologists' Union, 1910) species in the group. The first genetic study of the group (Johnson and Zink, 1985) found the North- and South American *olivaceus* monophyletic relative to the Central American *flavoviridis*, resulting in the current five-species taxonomy. Surprisingly, a recent study of mitochondrial DNA suggested the presence of at least six geographically and genetically distinct lineages (Slager et al., 2014), though basal nodes in the group were poorly supported.

Here we sequenced a genome-wide sampling of SNP's from museum specimens caught across the western hemisphere in order to assess the strength and distribution of species boundaries across the group. Specifically, we ask: (1) What is the optimal species delimitation scheme for partitioning diversity in the Red-Eyed Vireo Complex? (2) Do migrant species breeding in parapatry show evidence of gene flow after lineage divergence? And (3) Does introgression lead to erosion of neutral genetic differentiation among putative species?

1.3 Methods

1.3.1 Sampling and library preparation

We obtained frozen tissue samples from vouchered natural history museum specimens representing 40 individuals and 6 species of Vireo. These included four members of the Red-eyed vireo complex (*V. olivaceus, V. flavoviridis, V. altiloquus, V. magister*) and two outgroup taxa (*V. gilvus, V. plumbeus*) (Fig. 1, Supplementary Table 1). No tissue samples of *V. gracilirostris* (endemic to Noronha Island off the coast of Brazil) could be located, so this taxon was not included in our study. Southern and northern *V. olivaceus* were distinguished by subspecific identity in museum records, or by location and time of capture for any specimens lacking subspecific identification.

Whole genomic DNA was extracted using a Qiagen DNEasy spin-column extraction kit, following manufacturer instructions. Sequencing libraries were prepared following the ddRADseq protocol (Peterson et al., 2012). Briefly, we digested 300-500 ng of DNA per sample with NEB high-fidelity sbf1 and msp1 restriction enzymes. Barcoded adapters were ligated onto the resulting fragments and those in the 415-515 bp range were selected with a Blue Pippin Prep. Illumina flowcell annealing primers, PCR primers, and multiplexing indices were ligated to size-selected fragments, and the products amplified over 11 PCR cycles. We used a 1.5x ratio of AmPure XP beads to remove small DNA fragments between all steps. Amplification and size distribution were checked prior to sequencing with a qBit 2.0 fluorometer and a BioAnalyzer run. Samples were sequenced for 50 bp single-end reads on shared lanes (with other Passerine birds) across two runs of an Illumina Hiseq 2000.

1.3.2 Sequence Assembly

Raw sequencing reads were processed with pyRAD v. 2.17 (Eaton, 2014). PyRAD demultiplexes and quality-filters reads, then uses the Usearch algorithm (Edgar, 2010) to cluster reads into loci within samples and loci into stacks between samples. Stacks of putatively orthologous loci are then aligned with Muscle (Edgar, 2004) and output in a variety of sequence alignment formats for downstream analysis. We set a minimum read depth of 6 for calling consensus sequences within samples and used a clustering threshold of 0.90 for all Usearch runs. We filtered out all loci sharing heterozygotic sites across more than 8 individuals to avoid including paralogs in our sequencing alignment.

Because sample coverage – the proportion of sampled individuals sequenced for any given locus – is known to have a large effect on the total number of loci recovered (DaCosta and Sorenson, 2016; Huang and Knowles, 2014; Leaché et al., 2014), we prepared two sequence assemblies for downstream analyses by varying this parameter in pyRAD. The "MD10" alignment includes all loci sequenced for at least 90% of samples, while the "MD50" alignment includes loci sequenced for at least 50% of samples. To explore the source of missing data in our alignments we also used a Mantel Test to test for a correlation between pairwise genetic distance and the number of shared loci among samples.

Sequence alignments for concatenated phylogenetic analyses and structure input files were prepared with PyRAD's standard output options. STRUCTURE and Adegenet analyses used the MD50 alignment. SNAPP and RAxML were run on both MD50 and MD10 alignments, though only MD10 alignments were used for Bayes Factor Delimitation (BFD*). Both STRUCTURE and SNAPP input files include one random SNP per locus. For SNAPP, pyRAD's "unlinked_snps" output was converted to a three-state numeric input file (two alleles plus heterozygotes) suitable for analysis in SNAPP using custom R scripts written by Dr. Barbara Banbury and available online on the shinyphry webserver (https://rstudio. stat.washington.edu/shiny/phrynomics/). We

developed additional custom R scripts for visualizing patterns of missing data, writing D-test input files, summarizing D-test output, and plotting STRUCTURE results with consistent color matching (github.com/cjbattey/ radplots/). All analyses were conducted in the R programming language (Team and Others, 2013).

1.3.3 Phylogenetics

We ran two phylogenetic analyses on both the MD50 and MD10 alignments. First, we inferred a phylogenetic tree of concatenated full sequences (i.e. full RAD loci stripped of barcode, adapter, and restriction overhang sequences) in a maximum likelihood framework with the program RAxML v8 (Stamatakis, 2014). We used the GTR + Gamma model of sequence evolution and ran 1000 bootstrap iterations to assess support.

Next, we inferred a species tree in the program SNAPP v. 1.3 (Bryant et al., 2012), an add-on to the BEAST 2.2.0 package (Bouckaert et al., 2014). SNAPP requires the user to input the number of putative taxa and assign individual samples to these taxa. We initially assigned individuals to taxa based on nodes with at least 70% bootstrap support in the RAxML analysis (5 populations), and later re-ran the SNAPP analysis for the best-fitting BFD* model (6 populations, see Results). Because SNAPP models gene/species tree conflicts as the result of incomplete lineage sorting (ILS) rather than horizontal gene flow, we eliminated any individuals with more than 5% admixture in the best-performing STRUCTURE analyses from our SNAPP runs, resulting in the exclusion of two samples of V. olivaceus from Trinidad and Tobago. We used default values for forward and back mutation rates (3.33 and 5.08, respectively), and sampled the coalescence rate from a uniform infinite distribution. SNAPP analyses were run for one million generations, sampling every 10,000. Convergence was assessed through estimated ESS values and trace plots in Tracer v1.6 (Rambaut et al., 2014).

1.3.4 Clustering and Ordination

We used two unsupervised clustering algorithms to assign individuals to genetic clusters: STRUCTURE (Pritchard et al., 2000) and k-means clustering in the R package Adegenet (Jombart, 2008). For STRUCTURE analyses we adjusted the prior mean on F (parameter "FPRIORMEAN" in mainparams) to 0.1 (from the default value of 0.01) in order to reflect the higher expected divergence among named species. Analyses were run using the admixture model, correlated allele frequencies, and with a starting state based on population assignments from museum specimen records. We conducted 10 runs for each value of k between 2 and 8 and used the StructureHarvester web server to identify the value of k associated with the largest second-order change in marginal likelihood (Evanno et al., 2005; Earl and vonHoldt, 2012).

For Adegenet analyses we first conducted a Principal Components Analysis (PCA) on allele counts from the STRUCTURE input file, and then used k-means clustering to estimate the number of clusters and assign individuals to genotype clusters. We kept all PC axes for k-means clustering and inspected both population assignments and change in Bayesian Information Criterion (BIC) scores across values of k to select an optimal partitioning scheme for the group. PCA results were plotted using the first two PC axes and population assignments from k-means clustering (Fig. 1).

1.3.5 Admixture analysis

To test for introgression after the point of lineage divergence we calculated the D statistic ("ABBA/BABA") (Green et al., 2010) for all species pairs. D tests measure the imbalance in loci that conflict with the species tree, under the assumption that two types of discordant gene trees should occur with

equal frequency if ILS is the sole source of discordance. An imbalance in the distribution of discordant alleles is taken as evidence of introgression, and significance assessed by a Z score describing departure from a null mean derived from bootstrap replicates of the original data.

As in recent studies of plants (Eaton and Ree, 2013) and birds (Lamichhaney et al., 2015), we define a "test" in this context as asking "do populations X and Y show significant signs of introgression"? We calculated D for all unique combinations of individuals on a pectinate four-tip tree consistent with the SNAPP species tree for each test and applied a Holm–Bonferroni correction (Holm, 1979) to each p value to correct for multiple tests. Any combination of individuals returning less than 100 total discordant loci (including heterozygous sites) was removed from the test. We considered a population pair to show signs of introgression if any combination of individuals within the test gave a corrected two-tailed p value of less than 0.05.

1.3.6 Species delimitation with Bayes factors

We used Bayes Factor Delimitation in SNAPP (Grummer et al., 2014; Leaché et al., 2014) to rank species delimitation models in a multispecies coalescent framework. Briefly, BFD* consists of running SNAPP analyses on models with different numbers of species and assignments of individuals to species, estimating the marginal likelihood of each model, and ranking model fit among runs by comparing Bayes factors. In theory, BFD* provides a quantitative method for applying a flexible version of the genealogical species concept (Baum and Shaw, 1995) across multiple unlinked loci, in which the operational criteria for delimiting "species" is fit to a coalescent model with no gene flow.

For BFD* analyses we ran SNAPP on five species delimitation models under default parameters at a chain length of 50,000 (discarding the first 5000 as burn-in) for 48 steps. In this context "steps" refers to the different levels of power-posterior used in path sampling, and "chain length" refers to the length of the MCMC used to optimize parameters at each step. As in our species tree inference approach, we excluded samples with greater than 5% admixture in our best fitting STRUCTURE model from BFD* analyses, because SNAPP does not account for horizontal gene flow. BFD* analyses were run on the MD10 dataset only.

1.4 Results

1.4.1 RAD loci and missing data

After demultiplexing, trimming adapter and barcode sequences, and quality filtering in pyRAD, we recovered an average of 1.4e6 39-bp reads per individual. Usearch clustering at similarity 0.90 within individuals returned an average of 13,323 loci per individual. Two samples sequenced from relatively degraded DNA returned high levels of missing data (over two standard deviations above mean missing data percentage in the initial MD50 dataset; Supplementary Fig. 1) and were removed from the analysis, resulting in a final dataset of 38 individuals.

Sample coverage had a large impact on the total number of loci included in the alignment after sequence assembly. Our final "MD10" dataset consists of 938 loci, and the "MD50" dataset of 7799 loci. Total concatenated matrix lengths for MD10 and MD50 alignments are 36,582 and 304,161 base pairs, respectively. Mantel tests found that pairwise missing data were significantly correlated with genetic distance when all samples were analyzed ($p = 0.012$) but not when outgroups were removed ($p = 0.57$; Supplementary Fig. 1.2). This agrees with previous studies that failed to find significant correlations between missing loci and genetic distance at shallow (<10 my) timescales (Eaton and

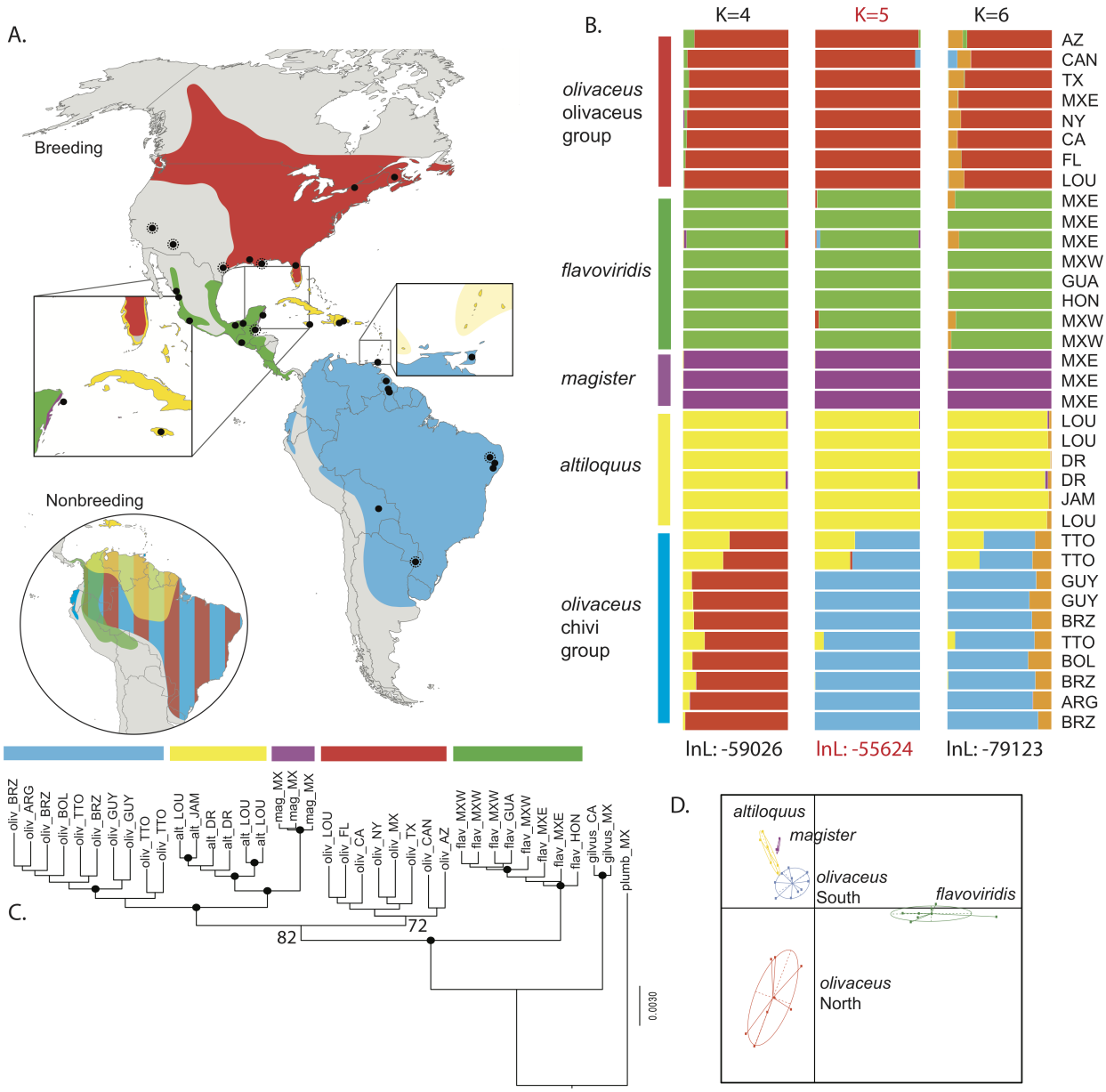

Figure 1.1: A: range map for breeding (top) and nonbreeding (bottom, circled) seasons, adapted from Birdlife International and Natureserve, 2013. Circled points representspecimens captured during the migration season. Magnified cutouts are provided for two regions of parapatry. B: STRUCTURE output for highest marginal-likelihood runs at k = 4 - 6. C: RAxML MD50 concatenated phylogeny. Numbers at nodes indicate bootstrap support, and circles represent bootstrap support > 90. D: PCA sample and population coordinates on the first two PC axes, using population assignments from k-means clustering.

Ree, 2013), suggesting that allelic dropout via mutation in restriction sites is not the primary source of missing data in ddRAD studies sampling at the population level in recently diverged groups.

1.4.2 Phylogenetics

Concatenation and species-tree analyses produced very similar topologies (Figs. 1.1 and 1.4) for both MD50 and MD10 alignments, though MD10 analyses had lower support values (Supplementary Figs. 1.3 and 1.4). The species tree is fully pectinate, with the Central American species *flavoviridis* representing the earliest-diverging extant lineage. Northern and southern *olivaceus* are paraphyletic, with South American breeders more closely related to the Caribbean taxa *altiloquus* and *magister* than their northern-hemisphere conspecifics.

SNAPP fully supported all nodes in the species tree using the MD50 alignment on both 5- and 6-population models (Fig. 1.4, Supplementary Fig. 5). For the MD50 alignment, RAxML bootstraps strongly supported the monophyly of a clade including southern *olivaceus*, *altiloquus*, and *magister*, but provided only moderate support for the monophyly of northern *olivaceus* and the sister relationship of *flavoviridis* to other taxa. In particular, some bootstrap replicates returned topologies in which northern /it olivaceus forms a paraphyletic grade sister to all ingroup taxa other than *flavoviridis*. This topology was also observed using the MD10 alignment in RAxML (Supplementary Fig. 4).

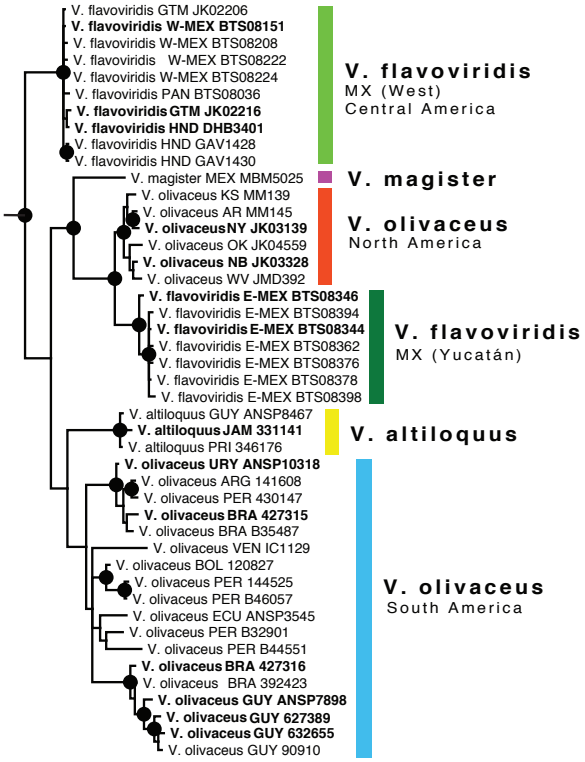

Figure 1.2: ND2 gene tree. Circles represent supported nodes. Bolded samples were also sequenced for nuclear SNP's. Bayesian posterior and ML bootstrap values are given at unsupported nodes.

The nuclear topology conflicted with that found in an earlier study of mitochondrial DNA in the clade (Slager et al., 2014) (Fig. 1.2); with the mtDNA topology finding *flavoviridis* polyphyletic in addition to *olivaceus*, and placing *magister* as sister to a combined clade of northern *olivaceus* and eastern *flavoviridis*

1.4.3 Clustering

STRUCTURE analyses strongly favored a five-population model that split northern and southern *olivaceus* and assigned individuals to the population cluster suggested by museum specimen records and concatenated phylogenetic analyses (Fig. 1.3; Table 1.1). The two samples of southern *olivaceus* placed outside the supported monophyletic clade in RAxML analyses were identified as hybrids between *olivaceus* and *altiloquus* in STRUCTURE output, a result that matches their geography: Trinidad and Tobago is the nearest point of contact between the ranges of *olivaceus* and *altiloquus* during the breeding season. Aside from these samples, STRUCTURE found very low levels of

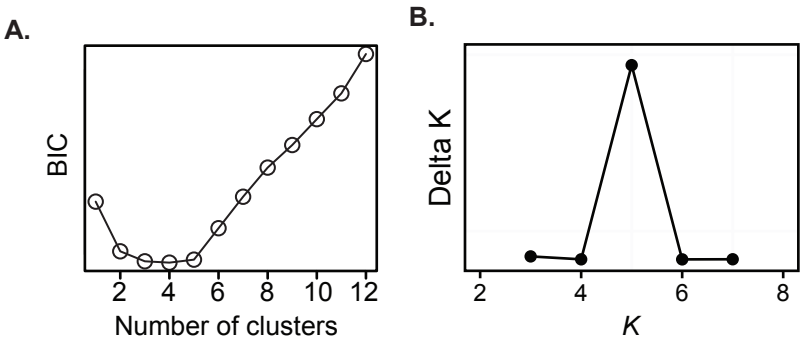

Figure 1.3: Summary of clustering results. A: BIC scores from k-means clustering in Adegenet. B: Evanno method output from STRUCTURE HARVESTER.

	Structure		Adegenet
K	Mean LnP(K)	Delta K	BIC
3	-63155.08	30.75	123.63
4	-61946.92	1.22	123.56
5	-55761.99	627.23	123.72
6	-94794.66	6.32	125.42
7	-72233.84	2.03	127.12

Table 1.1: Clustering analyses summary

admixture between species in the complex at k = 5, with no other individuals showing more than 5% admixture from a different putative species.

K-means clustering in Adegenet found that models with 3 - 5 clusters minimized BIC scores (Fig. 1.3; Table 1.1). In all k-means analyses, five was the highest value of k that matched results from existing taxonomy or mitochondrial DNA, with higher values placing individual *olivaceus* specimens in their own clusters. The first two PC axes cumulatively represent 13.2% of variance in the data. Distances among clusters using the first two PC axes were concordant with phylogenetic trees (Fig. 1). Interestingly, both clustering methods showed a tendency to lump northern and southern *olivaceus* when run at k = 4, rather than lumping any monophyletic clade identified in phylogenetic analyses. These results occurred in roughly half of STRUCTURE models run at k = 4 (others lumped *altiloquus* and southern *olivaceus*, or *altiloquus* and *magister*) and were consistently produced by k-means clustering, though in STRUCTURE all k = 4 models returned lower marginal likelihoods than five-population models.

1.4.4 Admixture

D statistics identified significant introgression between southern *olivaceus* and *altiloquus* in all tests that included one of the samples from Trinidad and Tobago. We also identified significant introgression between *olivaceus* and western *flavoviridis* in four combinations of individuals (Fig. 1.4; Table 1.2). In both cases, gene flow appears to be unidirectional (into *olivaceus*), as reciprocal tests failed to find significant introgression (though limited sampling in some areas may limit resolution of gene flow restricted to narrow hybrid zones). In the case of *flavoviridis*, all significant combinations involved west-Mexican individuals – conflicting with the mitochondrial topology that places east-

Mexican populations in a monophyletic clade with northern *olivaceus* and *magister* (Fig. 1.2). No tests with *magister* as the putative receptor lineage had over 100 discordant loci, reflecting the low genetic variability observed between samples of this micro-endemic species. Notably, for *olivaceus*, no combinations of individuals supported significant introgression between northern and southern populations.

Test	Number of loci	ABBA	BABA	Z range	Significant combinations
alt flav	3387	51	50	(0.03,1.69)	0/8
alt mag	2795	54	52	(0,1.11)	0/16
alt olivN	3148	48	43	(0.07,2.65)	030
alt olivS	3015	49	46	(0,2.89)	0/37
flav alt	3634	43	48	(0.24,1.83)	0/7
flav mag	3472	42	40	(0.09,0.68)	0/2
flav olivN	3515	39	44	(0.23,2.55)	0/14
flav olivS	3594	39	47	(0.06,1.86)	0/11
olivN alt	2357	63	65	(0.02,3.02)	0/126
olivN flav	**2211**	**59**	**63**	**(0.03,3.9)**	**4/153**
olivN mag	2218	63	65	(0,2.14)	0/62
olivN olivS	2203	59	59	(0,2.55)	0/205
olivS alt	**2318**	**53**	**65**	**0.02,5.71**	**23/172**
olivS flav	2476	57	58	(0.06,2.8)	0/99
olivS mag	2281	59	63	(0.03,2.46)	0/75
olivS olivN	2539	53	57	(0,2.88)	0/148

Table 1.2: D-Test results summary. Number of loci, ABBA and BABA are mean values for all combinations in a given test. Tests are given as the species assigned to P1/2 followed by P3 tips. Bolded rows indicate tests returning significant signal of introgression.

Model	lnL	2lnBF	Rank
Split *flavoviridis* + *olivaceus*	-6969.89	-	1
Split *olivaceus*	-6983.59	27.41	2
Split *flavoviridis*	-7154.83	369.88	3
Current taxonomy	-7168.87	397.96	4
Lump *olivaceus* + *altiloquus*	-7220.66	501.54	5

Table 1.3: BFD* results summary

1.4.5 Coalescent species delimitation

Bayes factor delimitation selected a model of 6 species, reflecting the major clades observed in the ND2 gene tree (Fig. 1.4; Table 1.3). This species delimitation scheme splits *olivaceus* between North and South American breeding populations, and /it flavoviridis between eastern Mexico and west Mexico + Central America. The second ranked model split *olivaceus* and retained a monphyletic *flavoviridis*, reflecting the clades in our concatenated RADseq tree. All models that did not split *olivaceus* were at least an order of magnitude worse performing than those that did (in terms of Bayes Factors), and splitting only *olivaceus* resulted in a much larger increase in marginal likelihood than splitting only *flavoviridis*. The mean ESS across all steps and all models was 326.7 (standard deviation = 211.0), suggesting that our chain length was sufficient to reach convergence.

1.5 Discussion

1.5.1 Migration, range, and gene flow

Dispersal ability and levels of genetic divergence across biogeographic barriers have generally been found to be inversely correlated in birds, with higher dispersing species experiencing more gene flow and lower levels of divergence among putatively allopatric populations (Smith et al., 2013). Long-distance migration represents the high end of the spectrum of dispersal abilities, suggesting that populations of migrant species are likely to experience high rates of gene flow, even when ranges are separated by substantial biogeographic barriers. Even in the Eurasian Blackcap (*Sylvia atricapilla*), a species for which migratory orientation is known to be heritable (Helbig, 1991), studies of up to 17 microsatellite loci have failed to find significant genetic structure among populations that vary in migratory behavior in the wild (Linossier et al., 2016; Mettler et al., 2013); suggesting that gene flow associated with incomplete philopatry may prevent divergence at selectively neutral loci. Even among well-recognized species of songbird, interspecific hybridization is relatively commonly reported (McCarthy, 2006). However, determining whether these events contribute significantly to the genetic makeup of extant species requires sampling extensively across the genome, which has historically limited the resolution of studies employing Sanger-sequencing approaches.

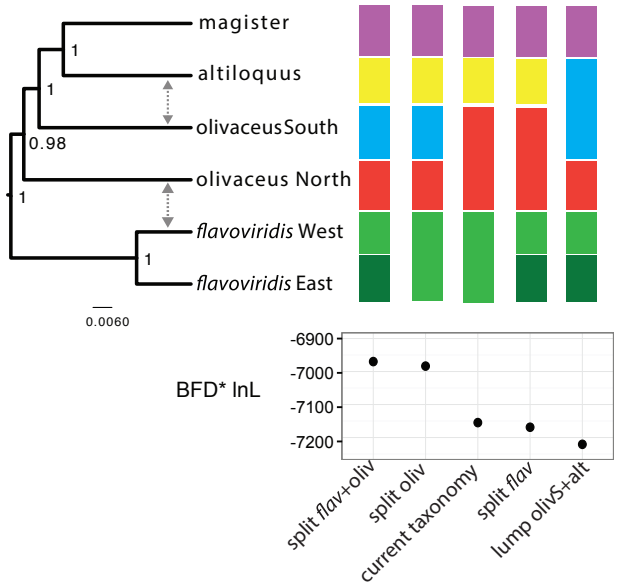

Figure 1.4: SNAPP species tree (MD50 alignment) and BFD* summary model summaries. Shaded bars depict species delimitation models tested in BFD*, with path-sampling marginal likelihoods provided below. Grey arrows indicate introgression events inferred by D tests.

Using genome-wide SNP's we observed significant introgression in two species pairs in the Red-Eyed Vireo Complex, but found that hybridization contributes little to the overall genomic makeup of most species. Intriguingly, we only observed introgression between species pairs for which the breeding ranges are separated by substantial range gaps. Among species breeding in sym- or parapatry (*olivaceus* and *altiloquus* in Florida; *olivaceus* and *flavoviridis* in the Darien, *magister* and *flavoviridis* on the Yucatán) we observed no introgressed individuals. In the cases where we did observe significant introgression it either occurred at very low levels suggestive of historic rather than contemporary gene flow (e.g. *flavoviridis* and northern *olivaceus*), or was limited to areas near the range boundaries of both species (*altiloquus* and southern *olivaceus*). Unlike the extensive homogenizing gene flow seen in *Acanthis* (Mason and Taylor, 2015), introgression in the Red-Eyed Vireo complex appears to contribute relatively little to the genomic makeup of these species despite occurring at detectable levels.

In addition to this broad view of gene flow in the group, our results provide the basis for several novel inferences of natural history and biogeography. First, putative *olivaceus* populations on the island of Trinidad appear to be hybrids between *olivaceus* and *altiloquus*. Although our sample size is quite limited, we observed significant introgression in all three TTO samples analyzed. The smallest gap between the breeding ranges

of *olivaceus* and *altiloquus* in the southern Caribbean is the approximately 80 miles of open ocean between the islands of Tobago and Grenada, and both island populations are reported to be sedentary (Cimprich et al., 2000). Contemporary hybridization would thus require either long-distance overwater dispersal by putatively sedentary birds, or double-breeding by overwintering *altiloquus* from the northern Caribbean. Although more extensive sampling is required to confidently infer the presence of a hybrid zone in the region, our observation should prompt further investigations of the nature of dispersal and migration in island populations of both species.

Second, the Yucatán vireo (*V. magister*) appears to represent an instance of speciation via loss of migration, as its ancestors are predominantly migratory and its range is adjacent to a known stopover location for its sister species (*altiloquus*) during fall migration (International, 2003). Migratory drop-off has been proposed to form a mechanism of speciation in *Sylvia* warblers (Voelker and Light, 2011) and *Catharus* thrushes (Outlaw et al., 2003). The recent finding that migration evolved primarily via temperate-breeding taxa extending their ranges to the south (Winger et al., 2014), coupled with the high species diversity of the tropics, suggests that loss of migration in tropical lineages is likely a common biogeographic pattern in neotropical birds.

1.5.2 Species delimitation

We found that the current five-species taxonomy under represents diversity in the Red-Eyed Vireo Complex. Both *olivaceus* and *flavoviridis* include genetically divergent lineages breeding in disjunct ranges (North and South America and Eastern and Western Mexico, respectively). In the case of *olivaceus*, genetics and life history both support splitting the species. Northern and southern hemisphere breeding populations are non-monophyletic, do not exchange genes at a level detectable in our data, and are characterized by variation in a heritable life-history trait that confers effective reproductive isolation between populations (e.g. direction and timing of migration; (Helbig, 1991; Pulido et al., 2001)). The apparent migratory divide in the species is an artifact of faulty taxonomy, not recent divergence, novel mechanisms of gene flow through resident populations, or the rapid evolution of migratory divides as documented in Barn Swallows (*Hirundo rustica*) (Garcia-Perez et al., 2013) and Eurasian Black-Caps (*Sylvia atricapilla*) (Bearhop et al., 2005).

V. flavoviridis is also structured between breeding populations in eastern and western Mexico and splitting the species was supported by BFD*, but other analyses suggested that these populations are at an earlier stage in the process of speciation than *olivaceus*. Although mitochondrial haplotypes are polyphyletic and entirely sorted between eastern and western Mexico (demonstrating that females migrating to breeding areas in the Sierra Madre Occidental and Sierra Madre Oriental have high fidelity to their breeding region), the species is monophyletic in nuclear SNP's. Clustering algorithms failed to distinguish eastern and western populations when run on the full dataset, and divergence between these populations in the species tree was much more recent than among any other putative species pair.

V. flavoviridis thus appears to be firmly within the "species/subspecies conundrum" (Huang and Knowles, 2016), in which different species delimitation criteria are likely to disagree on the taxonomic rank granted to hierarchically structured allo- or parapatric populations. In the absence of other data demonstrating reproductive isolation or intrinsic ecological or life-history variation among populations of *flavoviridis* (as seen in *olivaceus*), we take a conservative approach and propose elevating all populations of *olivaceus* breeding in South America to species status under the original name *Vireo chivi* (Vieillot, 1817), while retaining *V. flavoviridis* and its existing eastern and western subspecies (*V. f. flavoviridis* and *V. f. forreri*, respectively).

1.5.3 Mito - nuclear discordance

Topologies inferred from nuclear SNPs conflicted with mitochondrial DNA in three species that co-occur seasonally in eastern Mexico. Northern *olivaceus*, eastern *flavoviridis*, and *magister* form a monophyletic clade in ND2 sequences but are paraphyletic in nuclear SNPs. Two scenarios may explain this discordance: incomplete lineage sorting (ILS) of ancestral ND2 in the common ancestor of the complex, followed by fixation of a derived allele in eastern *flavoviridis* and *magister*; or introgression and mitochondrial capture among the parapatric species in eastern Mexico. Evidence distinguishing these scenarios is equivocal. In favor of hybridization, the discordant populations have (nearly) parapatric breeding ranges and overlap extensively in migration; while ILS is not expected to lead to any coherent geographic patterns. However, we found no evidence of nuclear introgression among northern *olivaceus*, eastern *flavoviridis*, or *magister*, as would be expected if hybridization was the cause of mtDNA discordance.

Although we cannot exclude either potential cause, we propose that the geographic and topological extent of discordance is more suggestive of past hybridization than ILS. At least one study has identified a case of complete mitochondrial capture despite statistically insignificant levels of nuclear introgression (Good et al., 2015). We hypothesize that hybridization may have initially transferred northern *olivaceus* mitochondrial haplotypes to *flavoviridis* and *altiloquus*, which subsequently became fixed in these populations through some combination of drift (aided by the reduced effective population size of the mitochondrial genome) and selection. Most existing evidence of interspecific hybridization and introgression has been drawn from studies analyzing a small number of loci, precluding accurate measurement of nuclear introgression (Toews and Brelsford, 2012). Our analysis supports the general findings of (Good et al., 2015) that nuclear and mitochondrial introgression can be entirely decoupled, and suggests that this system is a promising target for future investigations of the evolutionary dynamics of mitochondrial introgression.

1.6 Conclusions

We identified a cryptic species of songbird distinguished from its congeners by divergence in migratory direction and timing, and identified a set of unexpected hybrid individuals from putatively sedentary allopatric populations in the southern Caribbean. Our study demonstrates that post-divergence gene flow has relatively little impact on the overall genetic makeup of species in the Red-Eyed Vireo complex, despite occurring at detectable levels in two species pairs. Previous results from studies of mitochondrial DNA received partial support in our data, but did not reflect the genome-wide species tree of the group. Our study demonstrates the utility of genomic data for identifying cryptic species and generating novel natural history observations in groups with little phenotypic diversity.

1.7 Supplement and Data accessibility

Supplementary data associated with this article is available with the online version: http://dx.doi.org/10.1016/j.ympev.2017.056. Raw genomic data, sequence assembly parameters, and scripts for running analyses are available at: http://dx.doi.org/10.5061/ dryad.9b6p8.

1.8 Supplementary Tables

	Species	Name	Museum	Museum Number	Longitude	Latitude
1	*V. altiloquus*	alt_DR	AMNH	DOT-6385	-70.58	18.25
2	*V. altiloquus*	alt_LOU	LSU	21786	-89.56	29.98
3	*V. altiloquus*	alt_LOU	LSU	3814	-89.56	29.98
4	*V. altiloquus*	alt_LOU	LSU	13307	-89.56	29.98
5	*V. altiloquus*	alt_DR	AMNH	DOT-6379	-68.83	18.33
6	*V. altiloquus*	alt_JAM	FMNH	x331141	-77.69	18.43
7	*V. flavoviridis*	flav_GUA	UWBM	110069	-91.61	14.66
8	*V. flavoviridis*	flav_MXE	UWBM	101288	-90.68	18.64
9	*V. flavoviridis*	flav_MXE	UWBM	94425	-89.05	14.87
10	*V. flavoviridis*	flav_MXE	UWBM	101286	-90.68	18.64
11	*V. flavoviridis*	flav_MXW	UWBM	81437	-106.76	24.30
12	*V. flavoviridis*	flav_MXW	UWBM	83978	-106.31	23.36
13	*V. flavoviridis*	flav_MXW	UWBM	101086	-102.40	18.10
14	*V. flavoviridis*	flav_MXW	UWBM	101143	-102.31	18.17
15	*V. gilvus*	gilv_MX	UWBM	108071	-99.84	17.62
16	*V. gilvus*	gilv_CA	UWBM	110856	-119.23	36.96
17	*V. magister*	mag_MX	AMNH	DOT-18067	-87.00	20.34
18	*V. magister*	mag_MX	AMNH	DOT-18078	-87.00	20.34
19	*V. magister*	mag_MX	AMNH	DOT-18080	-87.00	20.34
20	*V. olivaceus*	olivN_MX	UWBM	100744	-89.79	20.84
21	*V. olivaceus*	olivN_NY	UWBM	110570	-74.43	44.00
22	*V. olivaceus*	olivN_LOU	UWBM	105387	-91.58	31.05
23	*V. olivaceus*	olivN_TX	UWBM	90182	-98.17	26.35
24	*V. olivaceus*	olivN_AZ	UWBM	78056	-109.18	32.87
25	*V. olivaceus*	olivN_CA	UWBM	109024	-118.23	37.40
26	*V. olivaceus*	olivN_FL	UWBM	109776	-81.88	29.26
27	*V. olivaceus*	olivN_CAN	UWBM	110755	-65.61	46.35
28	*V. olivaceus*	olivS_GUY	USNM	627389	-59.87	2.78
29	*V. olivaceus*	olivS_TTO	LSU	69311	-61.42	10.44
30	*V. olivaceus*	olivS_ARG	UWBM	70543	-55.09	-26.96
31	*V. olivaceus*	olivS_TTO	LSU	69419	-61.42	10.44
32	*V. olivaceus*	olivS_GUY	USNM	632655	-59.59	3.89
33	*V. olivaceus*	olivS_TTO	LSU	69665	-61.42	10.44
34	*V. olivaceus*	olivS_BRZ	FMNH	FMNH392424	-36.95	-8.81
35	*V. olivaceus*	olivS_GUY	ANSP	ANSP7898	-58.54	5.80
36	*V. olivaceus*	olivS_URU	ANSP	ANSP10318	-55.81	-32.56
37	*V. olivaceus*	olivS_BOL	FMNH	x334603	-62.08	-16.87
38	*V. olivaceus*	olivS_BRA	FMNH	x427316	-35.89	-35.89
39	*V. olivaceus*	olivS_BRA2	FMNH	x427315	-36.78	-9.57
40	*V. plumbeus*	plumb_MX	UWBM	98948	-115.57	36.15

Table 1.4: ddRAD specimens.

1.9 Acknowledgements

The authors thank Dr. Robert Bryson and Kevin Epperly for assistance with labwork and analyses. This manuscript was greatly improved by suggestions from two anonymous reviewers, and by comments from David Slager, Dr. Adam Leaché, Cooper French, and Ethan Linck. Dave Slager and Dr. Leaché also provided valuable assistance with implementing species delimitation analyses. Specimens analyzed in this paper represent the combined efforts of generations of collectors and curators without whom this work would be impossible. We thank the following institutions for providing specimen tissue samples: The Louisiana State Museum of Natural Science, American Museum of Natural History, Field Museum of Natural History, National Museum of Natural History, and the Academy of Natural Sciences at Drexel University.

Chapter 2

A Migratory Divide in the Painted Bunting (*Passerina ciris*)

2.1 Abstract

In the Painted Bunting (*Passerina ciris*), a North American songbird, populations on the Atlantic coast and interior southern United States are known to be allopatric during the breeding season, but efforts to map connectivity with wintering ranges have been largely inconclusive. Using genomic and morphological data from museum specimens and banded birds, we found evidence of three genetically differentiated Painted Bunting populations with distinct wintering ranges and molt-migration phenologies. In addition to confirming that the Atlantic coast population remains allopatric throughout the annual cycle, we identified an unexpected migratory divide within the interior breeding range. Populations breeding in Louisiana winter on the Yucatán Peninsula, and are parapatric with other interior populations that winter in mainland Mexico and Central America. Across the interior breeding range, genetic ancestry is also associated with variation in wing length, suggesting that selection may be promoting morphological divergence in populations with different migration strategies.

*Ethan Linck, Kevin Epperly, Cooper French, David Slager, Paul W. Sykes, and John Klicka were coauthors on the published version of this chapter, which appeared in the February 2018 issue of *The American Naturalist*: https://www.journals.uchicago.edu/doi/10.1086/695439. Cover and figure 1 illustration by Kevin Epperly.

2.2 Introduction

Migratory divides occur in regions where adjacent populations differ in the timing or route of seasonal migration. Because migratory behaviors have clear fitness impacts and are strongly heritable in several taxa (Helbig, 1991; Pulido et al., 2001; Quinn et al., 2000; Zhan et al., 2014), migratory divides are thought to represent a mechanism of lineage divergence in sympatry (Bearhop et al., 2005; Rolshausen et al., 2009). If hybrids between populations differing in migratory behavior attempt an intermediate strategy with lower fitness than either parental type, selection is expected to favor the evolution of mechanisms that reduce the probability of breeding across migratory types (Rohwer and Irwin, 2011). Recent studies combining genetic and individual tracking data have documented this scenario in a passerine bird (Delmore and Irwin, 2014), though reduced hybrid fitness has yet to be rigorously tested in the wild.

Understanding the role of seasonal migration in mediating gene flow among populations is also important in identifying distinct evolutionary and demographic units relevant to conservation and management. Because the level of immigration required to homogenize allele frequencies among populations is much lower than that expected to drive trends in population size (Waples and Gaggiotti, 2006), evidence of genetic differentiation is a conservative proxy for demographic independence. Migratory connectivity has long been recognized as a core criteria for delimiting fish stocks (Cadrin et al., 2014; Gillanders, 2002; Lipcius et al., 2008), but it has not been widely used in monitoring songbird populations. In part, this flows from our relatively sparse knowledge of variation in migratory behavior within most bird species (Faaborg et al., 2010).

The Painted Bunting (Passerina ciris) is a seasonal migrant to the southern United States with an interior breeding population that stretches across much of Mississippi, Louisiana, Arkansas, Oklahoma, Texas, and northern Mexico, and an eastern breeding population that hugs the Atlantic Coastline from northern Florida to Virginia (Figure 1.1). Two subspecies are currently recognized based on similarity in wing length and breast coloration – *P. c. ciris* breeding both along the Atlantic coast and in Louisiana and Mississippi, and *P. c. pallidior* breeding across the rest of the interior range (Storer, 1951). In addition to occupying allopatric breeding ranges, these populations pursue different molt-migration strategies: Atlantic coast populations fly south in September after molting on the breeding grounds, while interior populations depart the breeding grounds in July and molt during a migratory stopover in northwestern Mexico (Contina et al., 2013; Rohwer, 2013; Thompson, 1991).

Painted Buntings winter across Mexico, Central America, southern Florida, and the northern Caribbean, but connectivity between breeding and wintering ranges remains poorly characterized. While some researchers have suggested that the Atlantic coast population winters exclusively in southern Florida and on islands in the northern Caribbean (Thompson, 1991; Storer, 1951) others (e.g. Sykes et al. (2007)) propose that eastern birds may also winter in the Yucatán and farther south. Winter destinations of interior migrants are similarly unresolved. Based on wing length measurements and a qualitative analysis of breast coloration, Storer (1951) proposed that the birds breeding in Louisiana and Mississippi are trans-gulf migrants that winter on the Yucatán Peninsula, while birds that breed farther west use a circum-gulf route to sites elsewhere in Mexico and Central America. In a meta-analysis of specimen collection records, Linck et al. (2016) proposed that most interior buntings migrate in a counterclockwise pattern around Mexico after molting in Sonora and Sinaloa. A phylogeographic study of mitochondrial DNA variation across the species' breeding range showed significant population structure between Atlantic coast and interior populations (Herr et al., 2011); however, genetic data have not yet been used to identify links between breeding and wintering grounds.

Here we use genome-wide DNA sequence data and morphological analyses of museum specimens

to infer phylogeographic history and patterns of migratory connectivity in the species. Specifically, we 1) map migratory connectivity between breeding and wintering grounds, 2) test for morphological variation associated with divergent migratory strategies in the interior breeding range, and 3) estimate divergence times and rates of gene flow among populations. Our results highlight the contrasting roles of seasonal migration in driving both gene flow and genetic differentiation, and have significant conservation implications for an iconic but regionally declining songbird.

2.3 Methods

2.3.1 Genetic Sampling

We collected a total of 260 blood, tissue, and feather samples from across the breeding and wintering ranges of *P. ciris*, including 138 breeding-range samples previously analyzed in Herr et al. 2011. All Atlantic Coast samples were blood and feather samples taken during banding studies. Interior populations were represented by 148 frozen tissue samples of vouchered museum specimens held by the Burke Museum of Natural History and Universidad Nacional Autónoma de México.

Whole genomic DNA was extracted using Qiagen DNEasy extraction kits. We sequenced 1041 base pairs of the mitochondrial gene NADH dehydrogenase subunit 2 (ND2) from all samples using the primers and protocol described in Herr et al. 2011. Based on fragment size and DNA concentration, 95 samples were selected for reduced-representation library sequencing via the ddRADseq protocol (Tables 2.3 – 2.5; Peterson et al. (2012)). We used the digestion enzymes Sbf1 and Msp1 and a size-selection window of 415-515 bp. The resulting libraries were sequenced for 100 bp single-end reads on an Illumina HiSeq 2500.

Reads were assembled into sequence alignments using de-novo assembly in the program pyRAD v.3-0-65 (Eaton, 2014). We set a similarity threshold of 0.88 for clustering reads within and between individuals, a minimum coverage depth of 5 (per individual), and a maximum of 8 low-quality reads per site. To exclude paralogs from the final dataset, we filtered out loci with more than 5 heterozygous sites and those sharing a heterozygous site across more than 60 samples. We define "locus" throughout this manuscript as a cluster of sequence reads putatively representing the same 100-bp region downstream of an Sbf1 cut site. For clustering analyses, we required each locus to be sequenced in at least half of samples and randomly selected one parsimony-informative SNP per locus using a custom R script (https://github.com/slager/structure_parsimony_informative). Raw sequence data, assembly parameter files, specimen data, and scripts used to conduct all analyses are deposited in the Dryad Digital Repository: doi:10.5061/dryad.cp40s (Battey et al., 2017).

2.3.2 Genotype Clustering and Population Assignment

We used multivariate ordination and Bayesian coalescent clustering to identify genetically differentiated populations and assign wintering individuals to breeding regions. For multivariate analyses, we first conducted a principal components analysis using the covariance matrix of allele frequencies in each sample and then identified putative genetic clusters using k-means clustering in the R package Adegenet v2.0.1 (Jombart, 2008). We then cross-validated population assignments with discriminant analysis of principal components (Jombart et al., 2010) by randomly selecting half the samples in each k-means cluster, conducting a DAPC on these samples, and predicting the group assignments of remaining individuals with the "trained" DAPC model. Cross-validation analyses were repeated 1,000 times for k = 2-4 to estimate cluster assignment accuracy.

Bayesian clustering under a coalescent model with admixture was implemented in the program *structure*(Pritchard et al., 2000) using default priors, correlated allele frequencies, and a chain

length of 1,000,000. The first 100,000 steps were discarded as burn-in. We replicated structure analyses 5 times for each value of k=2-4, assessed change in marginal likelihood across values of k using Structure Harvester (Earl and vonHoldt, 2012), and used CLUMPP (Jakobsson and Rosenberg, 2007) to take the mean of permuted matrices across replicates after accounting for label switching. We estimated mean Fst using structure's parameterization, which follows Excoffier's definition (Excoffier, 2001) except for using a generalized model with separate drift rates for each population (Falush et al., 2003). We developed a custom web app for visualizing structure results (https://cjbattey.shinyapps.io/structurePlotter/; Battey (2017)), and summarized output of multivariate analyses using the R packages 'plyr' and 'ggplot2' Wickham (2016).

2.3.3 Mitochondrial DNA

Mitochondrial DNA analyses were conducted to identify the most likely breeding population of wintering samples collected in areas not well represented in ddRAD sequencing. We created 12 hypothetical population assignment schemes based on the results of nuclear SNP clustering, varying only the population assignment of samples from regions without nuclear SNP sequence data (Cuba, Bahamas, Costa Rica, and Nicaragua). Assignment schemes were compared by conducting an analysis of molecular variance (AMOVA; (Excoffier et al., 1992)) in the R package 'poppr' (Kamvar et al., 2014) and ranking models by the percentage of total variance explained by the population factor (following Herr et al. (2011)). We also inferred a median-joining haplotype network using the R package 'pegas' (Paradis et al., 2004) to visualize the distribution of haplotypes among putative populations.

2.3.4 Demographic Modeling

To estimate the timing of population splits and rates of gene flow among populations, we fit demographic models to the joint site frequency spectrum (SFS) of our nuclear SNP alignment in the program $\delta a \delta i$ v1.7 (Gutenkunst et al., 2010). We randomly selected 10 samples from each k-means population and called SNPs from this subset in pyRAD. PyRAD VCF files were then converted to $\delta a \delta i$'s input format using a custom R script (https://github.com/cjbattey/vcf2dadi). A single biallelic SNP was randomly selected from each locus, and the final dataset was projected to a size of 5 diploid individuals per population (proj=[10,10,10]). This yielded 3,044 SNPs from 4,128 loci.

We fit two 9-parameter demographic models representing the general phylogeographic history of the group (Figure S1). In both models a single ancestral population first splits into Eastern and Western groups, one of which then splits a second time to form the Central population. Migration is allowed between east+central and west+central populations after the final divergence event. The models differ only in whether eastern or western birds are sister to the central population. We ran 40 optimizations from randomized starting positions for each model, using the "optimize_log()" function in ai, and assessed uncertainty across 100 parametric bootstrap replicates of our original data (sampling each locus with replacement). We ranked models by calculating the difference in Akaike Information Criterion (AIC;(Akaike, 1987)) of the highest-likelihood parameter set for each model.

To convert model parameters to demographic values, we used the average genome-wide mutation rate of Geospiza fortis (3.44x10-9 substitutions/site/gen; (Nadachowska-Brzyska et al., 2015)) and a Passerina generation time of 1.63 years (Weir and Schluter, 2008). We estimated the effective sequence length for SNP calling by multiplying the total base pairs in our pyRAD alignment by the fraction of all SNPs incorporated in the SFS after projection.

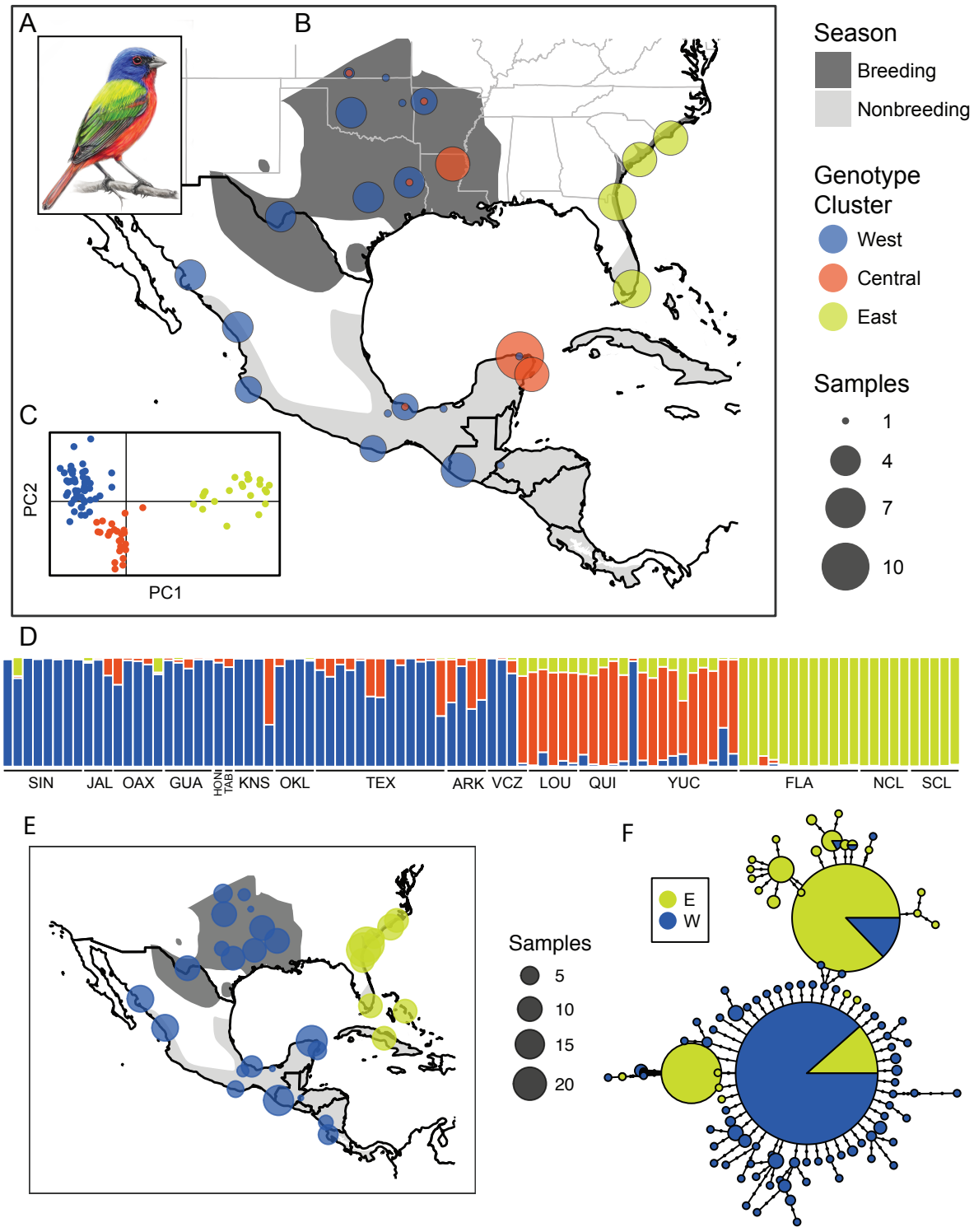

Figure 2.1: (A) Male P. ciris. (B) Sampling localities with points colored by k-means cluster and scaled to the number of samples. (C) Sample coordinates and k-means clusters on the first two PC axes. (D) Structure results at k=3, with each vertical bar representing a sample and the colors depicting the proportion of inferred ancestry from each population. (E-F) Mitochondrial DNA sampling map and haplotype network, colored by the best-performing AMOVA assignment scheme.

2.3.5 Morphology

Two previous studies documenting significant range-wide variation in Painted Bunting wing length concentrated primarily on differences between the allopatric coastal and interior breeding populations (Storer, 1951; Thompson, 1991). Here we focused on testing for morphological variation associated with the putative migratory divide within the interior breeding population, because variation in migration distance has previously been associated with wing length in both birds and butterflies (Altizer and Davis, 2010; Voelker, 2001). We measured wing chord and tarsus length (as a proxy for body size) of 56 museum specimens of adult male Painted Buntings collected in the breeding season (April-June). Wing chord was measured to the nearest 0.5mm with a metal stop ruler. Tarsus length was measured to the nearest 0.01mm with digital calipers.

We calculated and mapped mean values for both morphological traits for each unique locality recorded in the Burke Museum specimen database. After initial analyses found that wing chord and tarsus length were not significantly correlated (ordinary least squares regression, p=0.32, R2=0.02, df=54), we treated these variables as independent. We used a principal components analysis implemented in R to create a synthetic variable combining wing chord and tarsus length. We conducted ordinary least squares linear regressions to test for significant correlations between specimen longitude and each of wing length, tarsus length, and the first PC axis of wing and tarsus length. Finally, for the 21 specimens with both genomic and morphological data, we used linear regression to test for correlations between morphological traits and the proportion of "central" ancestry inferred by structure.

2.4 Results

2.4.1 Sequence Assembly

Illumina sequencing returned an average of 721,942 quality-filtered reads per sample. Clustering within individuals identified 36,497 putative loci per sample, with an average depth of coverage of 17. After clustering across individuals and applying paralog and depth-of-coverage filters, we retained an average of 9,010 loci per sample. As in most studies using RADseq-style reduced-representation libraries, we observed a large effect of missing data filtering on the size of our alignments, ranging from 238 to 25,434 unlinked SNPs for an all-samples-present vs. three-samples-present cutoff (DaCosta and Sorenson, 2016; Eaton et al., 2015; Leache et al., 2015). The final alignment used for clustering analyses included 3,615 unlinked parsimony-informative SNPs from 5,950 loci sequenced in at least 48 of 95 samples.

2.4.2 Genotype Clustering

In k-means clustering, BIC showed a single clear shift in slope at k=2, while structure returned the highest marginal likelihood at k=3 (Figure S2). Individual population assignments were similar in both methods, with k=2 models splitting breeding individuals between the Atlantic coast and interior breeding ranges, and wintering individuals between Florida and Mexico/Central America (Figure 1.1). At k=3, both methods cluster a group of breeding birds from Louisiana, eastern Texas, and Arkansas with wintering birds from the Mexican states of Yucatán and Quintana Roo. This "central" population appears to represent the easternmost end of a genetic cline across the interior breeding range, with samples from eastern Texas and western Arkansas falling in intermediate locations in principal components space and showing relatively high levels of admixture in structure analyses. Mean Fst in 3-population structure models was 0.11. Neither clustering method found geographically coherent clusters beyond k=3 (Figure S3-S4).

% Variance Explained by Population	*K*	Cuba	Bahamas	Central America
32.38	2	E	E	W
30.30	2	W	E	W
30.10	2	E	W	W
28.57	3	E	E	W
28.41	2	W	W	W
28.37	2	E	E	E
26.82	3	C	E	W
25.87	2	W	E	E
25.67	2	E	W	E
25.31	3	E	E	E
23.53	2	W	W	E
23.54	3	C	E	E

Table 2.1: Individual assignment schemes for mitochondrial DNA AMOVA's, ranked by the percentage of total variance explained by the population factor. Column K gives the total number of populations in the model. Columns with place names list a letter indicating the population assignment for each model.

Discriminant analyses estimated assignment probabilities over 0.99 for all individuals in both 2- and 3-population models. In cross-validation analyses, DAPC models trained on a random sample of half the individuals in each population correctly predicted the population assignment of an average of 99.7% of the remaining individuals at k=2, and 97.4% at k=3. DAPC cross-validation was also surprisingly robust at k values of 4 (85.5%) and 5 (76.2%), suggesting that denser population sampling could reveal further genetic structure in the interior breeding range.

2.4.3 MtDNA

The population assignment scheme that explained the highest percentage of total variance in AMOVA results grouped wintering birds from Cuba and the Bahamas with eastern breeding populations, and those from Costa Rica and Nicaragua with western breeding populations (Table 2.1). Models including a central population of Louisiana and Yucatán birds were consistently ranked lower than two-population models, but the highest-ranked 3-population model followed the same assignment scheme as the top model overall. All AMOVA results were significant ($p<0.01$). Haplotype networks were similar to those inferred using the breeding-season dataset of Herr et al. 2011, with the majority of western samples sharing a single common haplotype, and most eastern samples sharing one of two alternate haplotypes (Figure S5).

2.4.4 Demographic Modeling

Of the two demographic models we tested in $\delta a \delta i$, the model showing a sister relationship between west and central populations was best supported; however, the difference in AIC scores between models was just 0.78, providing weak support for this topology (Burnham and Anderson, 2004). In both models the internode distance between the first and second divergence events is relatively short (around 17% of the total tree depth), and the migration rate after the last divergence event is much higher between west and central populations than between the east and central popula-

tions (Table 2.2, Figure S6-S7). In the highest-likelihood parameter set, eastern and west+central populations diverged approximately 646,000 years ago, followed by central and west populations approximately 566,000 years ago. Gene flow is highest between central and west populations (3-9 migrants/generation), but also significant between east and central (1-3 migrants/generation). Although we observed relatively low uncertainty across bootstrap replicates, exact figures for divergence times and population sizes should be interpreted with some caution given uncertainty in the generation time and mutation rate. We note that our estimates of both population divergence times and migration rates are significantly higher than those estimated in a previous study of mitochondrial DNA under a 2-population model (Herr et al., 2011). Because migration and divergence time have opposing effects on the level of differentiation observed in modern samples, differences in parameter estimates could be caused by the presence of a "likelihood ridge" in which different combinations of these parameters produce similar likelihood scores. Alternatively, different inferences across genetic markers could be caused by biological phenomena, such as selective sweeps in mitochondrial genomes (Meiklejohn et al., 2007).

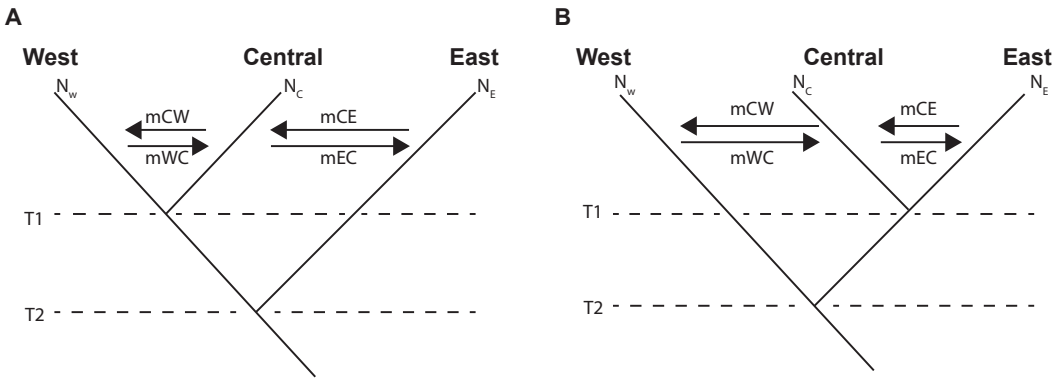

Figure 2.2: Demographic models fit in $\delta a \delta i$.

	((West, Central), East)	**((East, Central), West)**
Nref	92,806 (81,759 – 104,907)	116,157 (102,160 – 122,264)
Nw	592,365 (529,869 – 695,108)	572,601 (520,918 – 678,487)
Ne	43,702 (33,913 – 56,992)	41,627 (30,303 – 50,487)
Nc	256,213 (204,475 – 322,629)	304,896 (261,781 – 370,534)
T1	566,477 (524,704 – 606,666)	461,452 (418,442 – 537,264)
T2	646,705 (605,602 – 684,570)	680,303 (611,003 – 742,773)
Nm_wc	7.12 (5.51 – 8.81)	6.95 (5.61 – 9.14)
Nm_cw	3.75 (3.08 – 4.58)	3.57 (2.69 – 4.08)
Nm_ec	0.93 (0.87 – 1.05)	0.98 (0.90 – 1.06)
Nm_ce	1.82 (1.43 – 2.7)	2 (1.41 – 2.39)
LL_model	-620.58 (-660.74 – -607.95)	-620.97 (-659.70 – -612.73)

Table 2.2: $\delta a \delta i$ parameter estimates and 95% confidence intervals. Migration parameters ("Nm_") are the effective number of migrants per generation, with the receiving population listed first. "LL_model" is the log-likelihood of the model under optimized parameter sets.

2.4.5 Morphology

As in Storer 1951 and Thompson 1991, we observed a cline in wing length across Texas, Oklahoma, Arkansas, and Louisiana (Figure 2.2; Supplementary Table 3), with the shortest-winged birds in Louisiana. Wing chord ($p<0.01$, $R2=0.33$, $df=54$) and the first PC axis of wing chord and tarsus length ($p<0.01$, $R2=0.29$, $df=54$), but not tarsus length alone ($p=0.07$, $R2=0.04$, $df=54$), were significantly correlated with longitude. For the 22 specimens with both genomic and morphological data, wing chord ($p<0.01$, $R2=0.38$, $df=20$) and wing+tarsus PC1 ($p<0.01$, $R2=0.24$, $df=20$), but not tarsus length ($p=0.67$, $R2=0.01$, $df=20$), were also significantly correlated with the proportion of "central" ancestry in structure results.

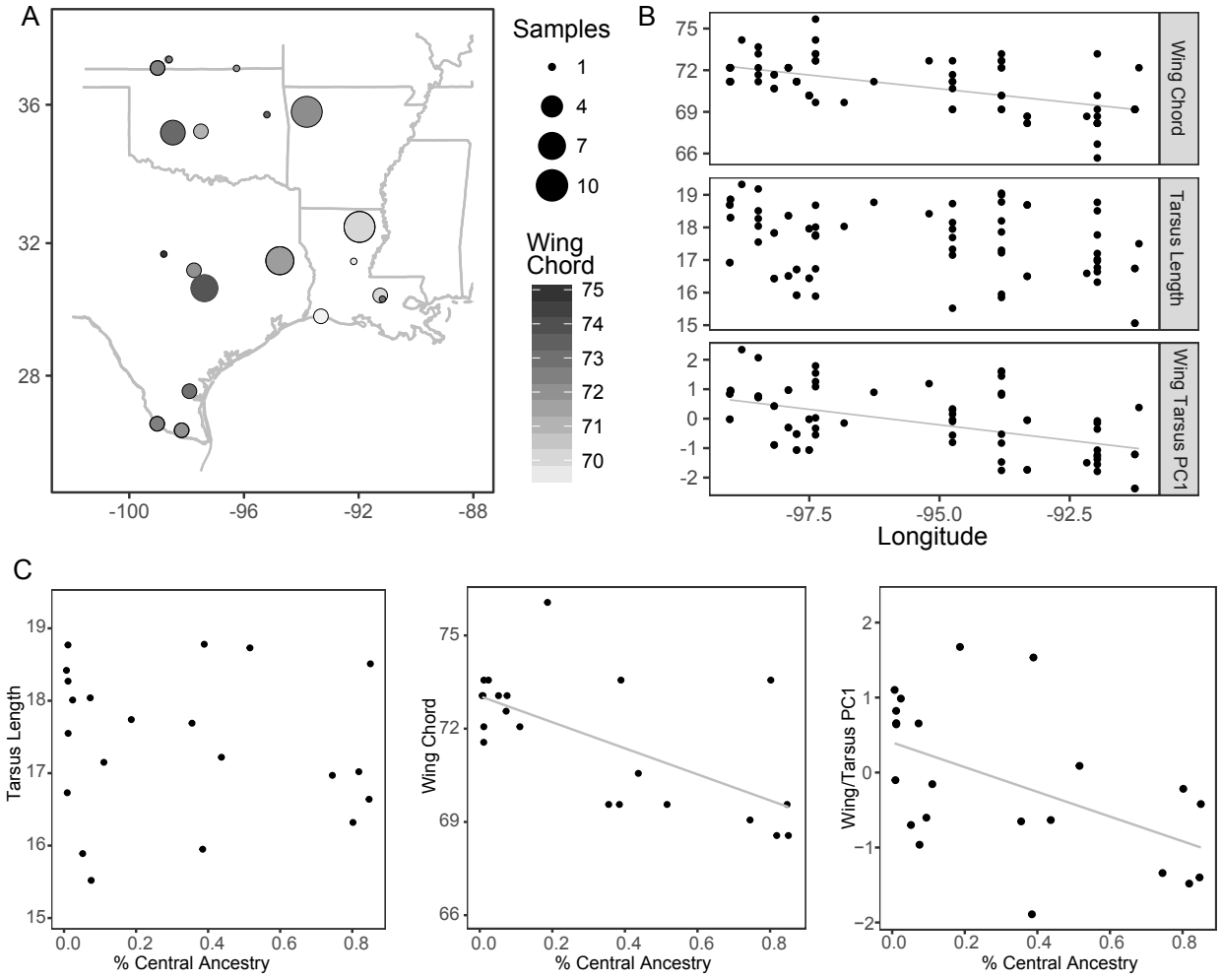

Figure 2.3: (A) map of specimen localities with points scaled by sample size and color graded by mean wing chord. (B) Linear regression of morphology as a function of longitude, with significant correlations shown as grey lines. (C) Linear regression of morphology as a function of the proportion of "Central" ancestry in 3-population Structure runs.

2.5 Discussion

2.5.1 Migratory Connectivity

Our study used thousands of genome-wide SNPs along with mtDNA sequences to produce the first range-wide map of migratory connectivity in Painted Buntings (Figure 2.1), yielding two major findings. First, we show that the Atlantic and interior breeding populations maintain allopatry year-round. Clustering analyses failed to group any individuals from the Atlantic Coast breeding population with any individuals from wintering localities in Mexico or Central America, a result consistent with previously hypothesized wintering range limits (Thompson 1991). Second, we found strong signals of a migratory divide that corresponds with the geographic break between *P. c. pallidior* and *P. c. ciris* in eastern Texas proposed by Storer (1951).

These genetically-conserved migratory programs may have important implications for the role of seasonal migration in shaping the evolutionary trajectory of populations. While seasonal migration can facilitate gene flow and promote homogenization among geographically segregated populations (Arguedas and Parker, 2000), it may also restrict gene flow and increase differentiation as differences in the timing and orientation of these seasonal movements begin to evolve among populations (Arguedas and Parker, 2000; Baker et al., 1994; Rohwer and Irwin, 2011). Our data indicate that the latter is occurring within Painted Buntings, potentially indicating the presence of incipient species. We believe this pattern reflects the consequences of extreme site fidelity across both the breeding and wintering range of the species.

Even in relatively well-studied taxa such as birds, the difficulty of tracking individuals and populations year-round has impeded research on many aspects of the ecology and evolution of migratory behavior (Webster et al., 2002). Painted Buntings are no exception, with previous studies proposing alternate migratory routes but failing to provide conclusive evidence of range-wide patterns. Based on similarities in plumage brightness and wing length, Storer (Storer, 1982, 1951) concluded that individuals breeding in the Mississippi Valley migrated directly across the Gulf of Mexico to winter on the Yucatán Peninsula. Prior to the present study, however, only a small number of mist-net captures on a single barrier island (Simons et al., 2004) and anecdotal observations from ships (e.g. Frazar (1881)) or oil platforms (Sullivan et al., 2009) provided support for trans-Gulf migration. Similarly, using banding records and differences in mean wing length between populations, Thompson (Thompson 1991) proposed that eastern Painted Buntings winter exclusively in southern Florida and the Caribbean, with western Painted Buntings wintering across Mexico and Central America. Unfortunately, a geolocator study (Contina et al. 2013) attempting in part to verify Thompson's hypotheses was hindered by low retrieval rates and stochastic individual behavior. By resolving these longstanding questions in Painted Bunting biology, our work joins Ruegg et al.'s (Ruegg et al., 2014) study of the Wilson's Warbler in using genomic data sampled across both breeding and wintering ranges to address recalcitrant questions in the natural history of avian migration.

2.5.2 Phylogeography

The discordance between the longitude of the Painted Bunting subspecies boundary (recognized on the basis of morphology), and the longitudinal limits of allopatric Atlantic and interior breeding populations has long vexed ornithologists (e.g. Storer 1951, Thompson 1991, Herr et al. 2011). Are current subspecies range limits an accurate reflection of phylogeographic structure and demographic independence, or do plumage and wing length characteristics reveal a hidden history of assortative mating? Our research corroborates both hypotheses. While our results broadly match the sole previous study of genetic variation within Passerina ciris based on a mtDNA marker (Herr et

al. 2011), the increased resolution afforded by genome-wide SNP data also reveals a previously undiagnosed genetic cluster consistent with morphological work by Storer (1951) and Thompson (1991) (Figure 2.1).

Niche modeling suggests that the east/west gap in the Painted Bunting distribution is well within the potential climatic envelope of the species (Shipley et al., 2013). Thus, we suggest that the contemporary distribution and genetic structure of the Painted Bunting is likely the result of one of three scenarios. 1) Adaptive morphological evolution related to migratory distance (as inferred from variation in wing length) may have been followed by the extinction of an intermediate portion of the ancestral range, potentially due to the fitness costs of trans-Gulf migration; 2) slow population expansion out of separate Late Pleistocene refugia (Johnson and Cicero, 2004); or, 3) a jump dispersal event (likely wind aided) in which a subset of interior trans-gulf migrants reached the Atlantic Coast (or Cuba), while retaining their the primary (north-south) migratory axis Greenberg and Marra (2005).

2.5.3 Implications for Conservation

The Atlantic coast population of Painted Buntings is a charismatic taxon restricted to a narrow strip of habitat heavily impacted by agricultural and residential development, and has consequently attracted substantial conservation efforts. The species as a whole is listed as "Near Threatened" on the IUCN red list, and is considered a "species of special concern" in the US Fish and Wildlife Service's Migratory Bird Program Strategic Plan (Fish et al., 2002). These designations are based primarily on data from the Breeding Bird Survey (BBS) finding that eastern populations have declined at an average rate of -1.17%/yr (95% CI -3.12, 0.08; (Sauer et al., 2017)), though trends in the region are not well supported because relatively few BBS routes are located in suitable habitat. In the west, BBS trends are highly variable, with populations apparently stable or expanding across northern Texas, Arkansas, and Oklahoma, while declining in Louisiana and Mississippi.

In contrast to earlier hypotheses of population structure in the species, which split buntings into eastern and western subspecies in eastern Texas (Storer 1951), or into two populations separated by the breeding range gap in the southeastern US (Thompson 1991, Herr et al. 2011), our analysis identified three populations (Figure 2.1). Re-examined in this framework, BBS survey data suggest that western populations are healthy and expanding in the north while central and eastern populations are declining. In Louisiana, BBS data identifies a well-supported decline of -1.85/yr (95% CI -2.95, -0.95) – a faster rate than in the east, where most conservation attention has focused. Eastern populations, meanwhile, have both the lowest effective population size and the lowest levels of gene flow with other populations. Though we are agnostic as to Thompson's 1991 hypothesis that they represent a separate species, the eastern population would likely qualify as a distinct population segment in the context of Endangered Species Act listing criteria (US Fish and Wildlife Service and National Marine Fisheries Service, 1996) if abundance declined significantly in the future. However, populations in the Mississippi alluvial valley region are also genetically differentiated from other Painted Buntings and show a more well-supported trend of population declines than eastern birds (mean -1.70/yr, 95%CI -2.86, -0.59), and should be monitored as a distinct demographic unit when analyzing survey data for the species.

2.6 Conclusions

We documented a migratory divide in the Painted Bunting using mitochondrial DNA, genome-wide SNPs, and morphological analyses. Breeding populations from Louisiana largely migrate to the Yucatán Peninsula, while those from central Texas and Oklahoma migrate first to molting grounds

in western Mexico and then to southern Mexico and Central America. Genetic data indicate that the Atlantic coast breeding population is allopatric from interior populations year-round; wintering only in southern Florida, the Bahamas, and Cuba. These populations have a deep history of divergence with gene flow, with all three splitting approximately 500,000-700,000 years ago but continuing to exchange an average of 1-9 migrants per generation after divergence. The genetic cline west of the Mississippi is also associated with variation in wing length; suggesting that selection may be promoting morphological divergence in populations with different migration strategies.

It is remarkable that basic life history traits of this charismatic and relatively well-studied species remain to be discovered, and points to an ongoing need for natural history observations to drive advances in both conservation and evolutionary biology. In this case our results support monitoring of the putatively declining central and eastern populations as separate demographic and evolutionary units for conservation purposes. This species is also a promising system for further studies of the genetic mechanisms underlying variation in molt and migration in songbirds. Painted Buntings were historically a common caged pet in the United States and have reportedly been bred in captivity (Greene, 1883), making them a potentially tractable system for conducting controlled crosses. Because Atlantic Coast and Interior breeding populations differ in the timing and location of molt in addition to migration (before vs. during fall migration, respectively), future studies in this system could provide insight into the mechanisms underlying temporal variation in the full annual cycle of Passerine birds.

2.7 Supplement and Data Availability

Supplementary Tables and figures are available with the published version on the website of *The American Naturalist*: https://www.journals.uchicago.edu/doi/10.1086/695439 . Raw genomic data and scripts for conducting all analyses are available on the Dryad digital data repository: https://doi.org/10.5061/dryad.cp40s .

2.8 Acknowledgements

We thank the staff and curators of the Burke Museum of Natural History and Universidad Nacional Autónoma de México for assistance with tissue loans, Yarrody Rodriguez for providing tail feathers for Cuban samples, and Darren Irwin for helpful comments on earlier versions of this manuscript.

Sample ID	State	Lat	Long	Source	Museum Number	MO	DY	YR
ARK_CAH143	Arkansas	35.80	-93.81	UWBM	101739	6	15	2005
ARK_CAH144	Arkansas	35.80	-93.81	UWBM	101740	6	15	2005
ARK_CAH156	Arkansas	35.80	-93.81	UWBM	101752	6	14	2005
ARK_CAH163	Arkansas	35.80	-93.81	UWBM	101758	6	14	2005
FLA_FL28W	Florida	25.49	-80.47	USGS	FL28W	1	23	2004
FLA_FL30W	Florida	25.49	-80.47	USGS	FL30W	1	23	2004
FLA_FLWN26	Florida	25.49	-80.47	USGS	FL_W_N26	1	23	2004
FLA_FLWN27	Florida	25.49	-80.47	USGS	FL_W_N27	1	23	2004
FLA_FLWN29	Florida	25.49	-80.47	USGS	FL_W_N29	1	23	2004
FLA_FLWN33	Florida	25.49	-80.47	USGS	FL_W_N33	1	23	2004
FLA_PB52307	Florida	30.44	-81.44	USGS	PB52307	8	2	2000
FLA_PB52314	Florida	30.44	-81.44	USGS	PB52314	8	2	2000
FLA_PB52315	Florida	30.44	-81.44	USGS	PB52315	8	2	2000
FLA_PB52329	Florida	30.41	-81.43	USGS	PB52329	8	3	2000
FLA_PB52330	Florida	30.41	-81.43	USGS	PB52330	8	3	2000
FLA_PB52335	Florida	30.44	-81.47	USGS	PB52335	8	4	2000
GUA_DHB4503	Retalhuleu	14.60	-91.61	UWBM	104172	1	10	2002
GUA_DHB4507	Retalhuleu	14.60	-91.61	UWBM	104176	1	10	2002
GUA_DHB4551	Retalhuleu	14.60	-91.61	UWBM	104220	1	10	2002
GUA_JK02010	Retalhuleu	14.60	-91.61	UWBM	109863	1	10	2002
GUA_JK02015	Retalhuleu	14.60	-91.61	UWBM	109868	1	11	2002
HON_JK00031	Copán	14.90	-88.90	UWBM	94126	4	15	2000
JAL_KSW3233	Jalisco	19.52	-105.07	UNAM	KSW 3233	10	18	1999
JAL_KSW3254	Jalisco	19.52	-105.07	UNAM	KSW 3254	10	21	1999
JAL_KSW3273	Jalisco	19.52	-105.07	UNAM	KSW 3273	10	22	1999
KNS_JK04545	Kansas	37.02	-96.26	UWBM	111618	5	28	2004
KNS_SAR7994	Kansas	37.26	-98.65	UWBM	90011	6	19	2009
KNS_SAR7995	Kansas	37.27	-98.61	UWBM	90012	6	19	2009
KNS_SAR7996	Kansas	37.26	-98.62	UWBM	90013	6	21	2009
LOU_CAH097	Louisiana	32.48	-91.97	UWBM	101694	6	2	2004
LOU_CAH098	Louisiana	32.48	-91.97	UWBM	101695	6	2	2004
LOU_CAH100	Louisiana	32.48	-91.97	UWBM	101697	6	2	2004
LOU_CAH140	Louisiana	32.48	-91.97	UWBM	101736	6	9	2005
LOU_JK04540	Louisiana	32.48	-91.97	UWBM	111613	6	2	2004
NCL_PB65637	North Carolina	33.86	-77.99	USGS	PB65637	8	28	2000
NCL_PB65639	North Carolina	33.86	-77.99	USGS	PB65639	8	28	2000
NCL_PB65648	North Carolina	33.87	-78.00	USGS	PB65648	8	29	2000
NCL_PB65655	North Carolina	33.87	-78.00	USGS	PB65655	8	29	2000
NCL_PB65658	North Carolina	33.87	-78.00	USGS	PB65658	8	29	2000
OAX_ASJ90	Oaxaca	18.08	-96.13	UNAM	ASJ 90	4	14	1995
OAX_DHB5578	Oaxaca	15.92	-97.08	UWBM	105252	1	16	2004
OAX_DHB5582	Oaxaca	15.92	-97.08	UWBM	105256	1	16	2004
OAX_DHB5715	Oklahoma	35.21	-98.48	UWBM	105390	5	25	2004
OAX_JMD069	Oaxaca	15.92	-97.08	UWBM	108268	1	16	2004
OKL_CAH081	Oklahoma	35.21	-98.48	UWBM	101678	5	25	2004

Table 2.3: ddRAD specimens – part 1/3.

Sample ID	State	Lat	Long	Source	Museum Number	MO	DY	YR
OKL_CAH090	Oklahoma	35.21	-98.48	UWBM	101686	5	25	2004
OKL_JK04554	Oklahoma	35.72	-95.20	UWBM	111627	5	27	2004
OKL_JMD369	Oklahoma	35.21	-98.48	UWBM	108580	5	25	2004
QUI_GLS10	Quintana Roo	20.44	-86.90	UNAM	GLS10	1	13	1995
QUI_GLS172	Quintana Roo	20.44	-86.90	UNAM	GLS172	3	17	1995
QUI_GLS23	Quintana Roo	20.44	-86.90	UNAM	GLS23	1	15	1995
QUI_MGL19	Quintana Roo	20.44	-86.90	UNAM	MGL19	1	15	1995
QUI_PEP2969	Quintana Roo	20.44	-86.90	UNAM	PEP2969	10	12	1994
SCL_PB65537	South Carolina	32.72	-79.99	USGS	PB65537	8	18	2000
SCL_PB65545	South Carolina	32.72	-79.99	USGS	PB65545	8	18	2000
SCL_PB65556	South Carolina	32.72	-79.99	USGS	PB65556	8	18	2000
SCL_PB65557	South Carolina	32.72	-79.99	USGS	PB65557	8	18	2000
SCL_PB65564	South Carolina	32.72	-79.99	USGS	PB65564	8	18	2000
SIN_CSW7732	Sinaloa	26.28	-108.80	UWBM	90608	9	28	2010
SIN_CSW7736	Sinaloa	26.28	-108.80	UWBM	90612	9	28	2010
SIN_CSW7737	Sinaloa	26.28	-108.80	UWBM	90613	9	28	2010
SIN_CSW7763	Sinaloa	26.28	-108.80	UWBM	90637	9	30	2010
SIN_EAG016	Sinaloa	23.25	-105.75	UWBM	81416	7	17	2005
SIN_EAG024	Sinaloa	23.25	-105.75	UWBM	81424	7	18	2005
SIN_EAG032	Sinaloa	23.25	-105.75	UWBM	81432	7	18	2005
SIN_RCF2610	Sinaloa	23.25	-105.75	UWBM	81134	7	17	2005
TAB_CAM318	Tabasco	18.36	-92.56	UNAM	CAM 318	3	11	1996
TEX_BTS05071	Texas	29.59	-103.00	UWBM	100190	5	28	2005
TEX_CAH087	Texas	30.66	-97.38	UWBM	101683	6	26	2004
TEX_CAH146	Texas	31.48	-94.75	UWBM	101742	6	7	2005
TEX_CAH149	Texas	31.48	-94.75	UWBM	101745	6	6	2005
TEX_CAH153	Texas	31.48	-94.75	UWBM	101749	6	6	2005
TEX_CAH155	Texas	29.59	-103.00	UWBM	101751	5	29	2005
TEX_CAH161	Texas	31.48	-94.75	UWBM	101756	6	6	2005
TEX_CAH162	Texas	31.48	-94.75	UWBM	101757	6	6	2005
TEX_CAH170	Texas	29.59	-103.00	UWBM	101765	5	29	2005
TEX_CAH177	Texas	29.59	-103.00	UWBM	101772	5	28	2005
TEX_JK04518	Texas	30.66	-97.38	UWBM	111592	6	26	2004
TEX_JK04519	Texas	30.66	-97.38	UWBM	111593	6	26	2004
TEX_JK04563	Texas	30.66	-97.38	UWBM	111636	6	27	2004

Table 2.4: ddRAD specimens – part 2/3.

Sample ID	State	Lat	Long	Source	Museum Number	MO	DY	YR
VCZ_TUX1094	Veracruz	18.48	-95.03	UNAM	TUX 1094	10	18	1994
VCZ_TUX1107	Veracruz	18.48	-95.03	UNAM	TUX 1107	10	25	1994
VCZ_TUX1402	Veracruz	18.48	-95.03	UNAM	TUX 1402	4	27	2003
VCZ_TUX204	Veracruz	18.48	-95.03	UNAM	TUX 204	4	9	1994
YUC_BRB849	Yucatán	21.52	-87.70	UWBM	99969	1	13	2009
YUC_BRB875	Yucatán	21.52	-87.70	UWBM	99995	1	13	2009
YUC_BRB878	Yucatán	21.52	-87.70	UWBM	99998	1	14	2009
YUC_BRB883	Yucatán	21.52	-87.70	UWBM	100003	1	14	2009
YUC_BRB893	Yucatán	21.52	-87.70	UWBM	100013	1	14	2009
YUC_BRB928	Yucatán	21.52	-87.70	UWBM	100045	1	14	2009
YUC_BRB941	Yucatán	21.52	-87.70	UWBM	100057	1	15	2009
YUC_BRB942	Yucatán	21.52	-87.70	UWBM	100058	1	15	2009
YUC_CAM013	Yucatán	21.51	-87.67	UNAM	CAM 013	3	9	1995
YUC_CAM109	Yucatán	21.51	-87.67	UNAM	CAM 109	3	19	1995
YUC_CAM31	Yucatán	21.51	-87.67	UNAM	CAM 31	3	10	1995

Table 2.5: ddRAD specimens – part 3/3

.

Chapter 3

Evidence of Linked Selection on the Z Chromosome of Hybridizing Hummingbirds

3.1 Abstract

Levels of genetic differentiation vary widely along the genomes of recently diverged species. What processes cause this variation? Here I analyze geographic population structure and genome-wide patterns of variation in the Rufous, Allen's, and Calliope Hummingbirds (*Selasphorus rufus/sasin/calliope*) and find evidence that linked selection on the Z chromosome drives patterns of genetic differentiation in a pair of hybridizing species. Demographic models, introgression tests, and genotype clustering analyses support a reticulate evolutionary history consistent with divergence during the late Pleistocene followed by gene flow across migrant Rufous and Allen's Hummingbirds during the Holocene. Relative genetic differentiation (*Fst*) is elevated and within-population diversity (π) depressed on the Z chromosome in all interspecific comparisons. The ratio of Z to autosomal within-population diversity is much lower than that expected from population size effects alone, and Tajima's D is depressed on the Z chromosome in *S. rufus* and *S. calliope*. These results suggest that conserved structural features of the genome play a prominent role in shaping genetic differentiation through the early stages of speciation in northern *Selasphorus* hummingbirds, and that the Z chromosome is a likely site of genes underlying behavioral and morphological variation in the group.

3.2 Introduction

Populations become more different over time due to a combination of mutation, drift, and selection, but the relative importance of these factors in shaping modern biodiversity is contentious. Are differences among species and populations shaped primarily by isolation and drift, or by selection? Variations on this debate occur at all levels of biological hierarchy – from population genetic studies asking if genetic variation is adequately explained by neutral processes (Kern and Hahn, 2018; Kimura, 1968), to phylogeographic studies that ask if speciation has proceeded with or without gene flow (Nosil, 2008), to macroevolutionary analyses that seek to estimate the ratio of sympatric to allopatric speciation by studying range overlap in across whole taxonomic classes (Phillimore et al., 2008). At the level of the genome, a similar question arises: what process explains variation in differentiation across the genome?

Recent studies analyzing whole genome data from, among others, hominins (Phillimore et al., 2008), bears (Kumar et al., 2017), fruit flies (Cooper et al., 2018), butterflies (Heliconius Genome Consortium, 2012), fish (Schumer et al., 2018), and songbirds (Toews et al., 2016) indicate that hybridization is relatively common in animals and is not restricted to recently diverged sister lineages. In some cases morphologically and behaviorally differentiated populations hybridize to the extent that the vast majority of the genome is homogenized and only a few small regions are differentiated across species (Toews et al., 2016; Fontaine et al., 2015). Two explanations are typically offered for this pattern: selection against hybrid ancestry in certain regions of the genome leading to local reduction in gene flow in "genomic islands of speciation" (Nosil et al., 2009), or reductions in diversity caused by linked selection within isolated populations leading to local elevation of relative differentiation in regions of low recombination (Cruickshank and Hahn, 2014). Though the debate around which of these scenarios is more common has sometimes set them in opposition, both imply that the core processes driving variation in differentiation across the genome are natural selection and recombination.

Studies of genetic variation within species also support a prominent role for selection and recombination. In the Passenger and Band-Tailed Pigeons, regions of elevated nucleotide diversity (π) occur in parts of the genome with high recombination, and the strength of this relationship appears to vary with effective population size (Murray et al., 2017). Because selection should be more effective in larger populations and will remove diversity from larger chunks of the chromosome in regions with low recombination, these results suggest that linked selection explains much of the variation in diversity across the genome of these species.

One region in which the impacts of selection should be particularly prominent are the sex chromosomes. In birds, which have a ZW sex chromosome system (females are ZW), Z-linked alleles have been linked to sexually selected plumage traits involved in mate selection (Toews et al., 2016; Saether et al., 2007). The avian Z chromosome is also known to have a faster mutation rate (around 1.1x; reviewed in Irwin (2018)), and a lower recombination rate than autosomes because most of the chromosome does not recombine in females. Both purifying selection and disruptive selection on traits important in speciation are thus likely to be more common on the Z chromosome, and are expected to remove diversity from larger genomic regions. However, sex chromosomes also have lower effective population sizes than autosomes (3/4 for the Z; 1/4 for the W), and represent a tiny fraction of the full length of the genome in most species. These factors may limit the effectiveness and frequency of selection and instead favor drift as a main role driving Z chromosome differentiation.

Here I investigate the impacts of geographic isolation and linked selection in creating patterns of genetic differentiation in *Selasphorus* hummingbirds in western North America and find evidence of linked selection in driving regions of elevated relative differentiation, with a particularly strong effect

on the Z chromosome. I first test for population structure and isolation-by-distance by comparing genetic variation in individuals caught on the breeding range and during migration to determine if populations retain geographic structure through migration. I then estimate the phylogeographic history of the group by fitting demographic models to the joint site frequency spectrum inferred from whole-genome sequencing data, and use a genome scan approach to identify specific regions of the genome differentiated between and within species. Last I test for variation in genetic diversity on the Z chromosome and autosomes, and compare relative divergence and within-population diversity across multiple population pairs representing a spectrum of divergence times.

3.2.1 Natural History of Northern *Selasphorus* Hummingbirds

The Rufous (*S. rufus*) and Allen's (*S. sasin*) hummingbirds are the most recently diverged members of the "bee hummingbird" clade that colonized temperate North America roughly 5-10 million years ago (McGuire et al., 2014; Licona-Vera and Ornelas, 2017). Both species are small-bodied with rufous sides, pale bellies, and (for males) an iridescent orange-red gorget. In the field most individuals are indistinguishable, with reliable morphological traits visible without capture limited to a completely rufous back vs a mixed green and rufous back in adult males and a slightly narrower outer tail feather in *S. sasin* (Pyle et al., 1997). Females and juveniles are generally indistinguishable unless they can be caught and measured.

S. rufus are obligate migrants that breed in riparian and wet conifer forests across the Pacific Northwest from southern Oregon to central Alaska, extending east to western Montana and the Canadian Rockies. *S. sasin* includes two subspecies, with the migratory *S. s. sasin* breeding in a narrow strip along the California coast from Los Angeles to the Oregon border and the sedentary *S. s. sedentarius* occupying the Channel Islands and parts of urban southern California year-round (Healy and Calder, 2006). Migratory populations of both species winter primarily in central Mexico, but the specific regions and timing of seasonal movements on the wintering grounds are poorly described. In recent years Rufous Hummingbirds have also been increasingly observed wintering along the Gulf Coast of the southern US (Hill et al., 1998).

Phylogenetic studies of the Trochilidae (McGuire et al. 2014) and Bee Hummingbird clades (Licona-Vera and Ornelas, 2017) identify the rufous and Allen's hummingbirds as sister to the *calliope* hummingbird (*sasin*) in the "Northern *Selasphorus*" clade, which diverged from a primarily Central American group including the broad-tailed hummingbird (*S. platycercus*) 4.5 – 2.5 million years ago. One previous study examined microsatellite variability in rufous hummingbirds across British Columbia and found evidence of a modestly structured population (Bailey et al. 2013), but no study has examined structure across the full breeding range. Population genetic structure within the Allen's hummingbird has not been previously studied. Note that similar observations of low autosomal and high Z chromosome *rufus* x *sasin* differentiation to those observed here were first reported by a separate research group in a conference presentation (Brelsford et al., AOU Tucson 2018).

3.3 Methods

3.3.1 Sampling

I gathered tissue samples from natural history specimens of 85 *S. rufus*, 6 *S. sasin sasin* from the San Francisco Bay Area, 5 *S. sasin sedentarius* from the Channel Islands, and 8 *S. calliope* (Supplementary Table S2 – S4). All *S. sasin* and *S. calliope* were collected during the breeding season. *S. rufus* samples included 50 individuals collected between March and June along a north-south axis

from Oregon to Alaska, and 35 individuals collected during fall migration along an east-west axis from southern California through Texas. DNA was extracted with a Qiagen DNEasy extraction kits and quantified with a qubit BR kit. All samples were prepared for reduced-representation library sequencing via the double-digestion restriction-associated digest protocol (ddRADseq; (Peterson et al., 2012)); using the digestion enzymes sbf1 and msp1 and a size-selection window of 350-900bp. Pooled libraries were then sequenced for 150bp single-end reads on two lanes of a Hiseq 2500 at the UC Berkeley Vincent J Coates sequencing lab.

40 individuals were selected for low-coverage whole-genome sequencing based on fragment size and preliminary population structure analyses of ddRAD data. These samples included 4 *S. sasin sasin*, 4 *S. sasin sedentarius*, 7 *S. calliope*, and 25 *S. rufus* (8 breeding and 17 migrants). WGS library prep followed the standard illumina protocol for 450-550bp fragments using Truseq nano prep kits, but employed a Bioruptor rather than a Covaris for the initial sonication step. Fragment lengths and concentrations were assayed throughout the library preparation using a bioanalyzer. Twenty uniquely barcoded individuals were pooled in equimolar amounts for each sequencing lane, and samples were sequenced for paired-end 150bp reads on a Hiseq 3000.

3.3.2 Sequence Assembly

ddRAD libraries were demultiplexed using the "-s 1" function of pyRAD (v 1.8; (Eaton, 2014)). I first checked for contamination by aligning all reads to a concatenated fasta file including the human genome and twenty common bacterial and fungal genomes and removing any reads that aligned to this contaminant set at mapping quality > 10 (no samples returned over 0.5% contaminant alignment). Remaining reads were then aligned to a high-quality reference genome of the Anna's Hummingbird (*Calypte anna*) based on a combination of illumina and Pac-Bio long-read sequencing (*Calypte anna*, (Korlach et al., 2017)) using the program Bowtie2 (Langmead and Salzberg, 2012). Reads with a mapping quality below 30 were dropped from the analysis. I used STACKS v2.0 (Catchen et al., 2013) to assemble aligned reads into orthologous loci and call SNP's across individuals. Our final dataset included 11,762 SNP's from 6,530 loci sequenced in at least 90% of individuals.

SNP calling for whole-genome sequence data followed the best practices workflow described in the GATK documentation (https://software.broadinstitute.org/gatk/best-practices/). AdapterRemoval v2 (Lindgreen, 2012) was used to trim adapters and merge overlapping paired reads, and all reads were aligned to the contaminant reference described above. Reads aligning to the contaminant reference with a MQ > 10 were dropped. I then aligned all reads to the Korlach et al. 2017 *C. anna* reference genome using Bowtie2. I sorted and indexed bam files with samtools, marked optical and PCR duplicates using the "MarkDuplicates" tool in Picard (http://broadinstitute.github.io/picard/). Two approaches were used to prepare alignments for for downstream inference - static SNP calling with the "UnifiedGenotyper" tool in GATK (McKenna et al., 2010), and genotype likelihood estimation with ANGSD (Korneliussen et al., 2014). Called SNPs were used to confirm sexes of individuals (by comparing read depth on contigs mapping to the Z chromosome), estimate population trees, and infer single-species demographic histories; while genotype likelihoods were used to calculate windowed summary statistics across the genome.

The use of two approaches for SNP calling in whole-genome data was necessary because quality filtering genotypes with low coverage sequencing data likely eliminates some true SNP's such that the effective sequence length used for SNP calling is lower than the length of the reference genome. Consequently analyses relying on full sequence information (e.g. π) are biased downward in static calls. In both cases sites in the top 2.5% of average read depth were dropped to avoid including paralogs in the alignment. After manually inspecting diversity estimates and read depths across

the genome, two contigs on chromosome 4 were also dropped as they appear to include paralogs or copy number variants that were not removed by previous filters. Static calls were filtered in vcftools (Danecek et al., 2011) to retain only biallelic sites with no missing data and a site quality of at least 30, resulting in a final set of 5,688,922 variants with a mean sequencing depth of 4.35x. Genotype likelihoods and site frequencies estimates were calculated from bam files in ANGSD using the options "-remove_bads -unique_only -minMapQ 20 -minQ 20 -only_proper_pairs 1", following those implemented in (Delmore et al., 2018).

3.3.3 Phylogenetics and Population clustering

I first estimated a population tree for the concatenated sequence matrix of ddRAD samples in RAxML v8.0 (Stamatakis, 2014), using a GTRGAMMA model of sequence evolution and estimating uncertainty with 100 bootstrap replicates. The called SNP alignment from whole-genome resequencing was also used to estimate a neighbor-joining tree in the R package 'APE' (Paradis et al., 2004), using a k80 model when calculating genetic distances. Last, a population tree was estimated from whole-genome SNP's in Treemix (Pickrell and Pritchard, 2012) with *S. sasin sasin* and *S. sasin sedentarius* modeled as separate populations and allowing 2 migration edges. *S. calliope* was set as the outgroup for treemix analyses and SNP's were grouped in bins of 1000 to account for linkage disequilibrium.

I then focused on describing population structure in *S. rufus* and *S. sasin* with principal components analysis (PCA) and model-based clustering in the program *structure* (Pritchard et al., 2000). PCA's were conducted using the R package 'Adegenet' (Jombart, 2008) on the covariance matrix of SNP's across *rufus* and *sasin* ddRAD samples, with missing data replaced by the mean allele frequency across all samples.

Structure analyses are biased by inclusion of singletons (Linck and Battey, 2017) and by unequal sample sizes across populations (Falush et al., 2016), so I first filtered out all sites with a minor allele count lower than 3 using custom R scripts (see https://github.com/cjbattey/maf/maf_functions.R)) and then ran separate *structure* analyses for *sasin* + breeding *rufus* samples and *sasin* + migrant *rufus* samples. *Structure* analyses were run using the admixture model with correlated allele frequencies for 100,000 MCMC steps with 10,000 steps of burn-in for five replicates under different starting seeds at K values of 1-4. I then used structure harvester (Earl and vonHoldt, 2012); (http://taylor0.biology.ucla.edu/structureHarvester/) to rank K values by second-order change in marginal likelihood (Evanno et al., 2005).

To test for isolation by distance within *S. rufus*, I assessed correlations between genetic and geographic distance matrices using a Mantel test. Genetic distances were estimated assuming a k80 model of sequence evolution in the R package 'ape' (Paradis et al., 2004). As a secondary test of IBD, I also used linear regression to test for correlations between the first principal component of the allele frequency matrix and latitude (for breeding samples) or longitude (for migrants). Results from all analyses were plotted using the R packages 'ggplot2' (Wickham, 2016), 'maps' (Becker et al., 2013), and 'cowplot' (Wilke, 2016) in R v3.4.1 (Team and Others, 2013).

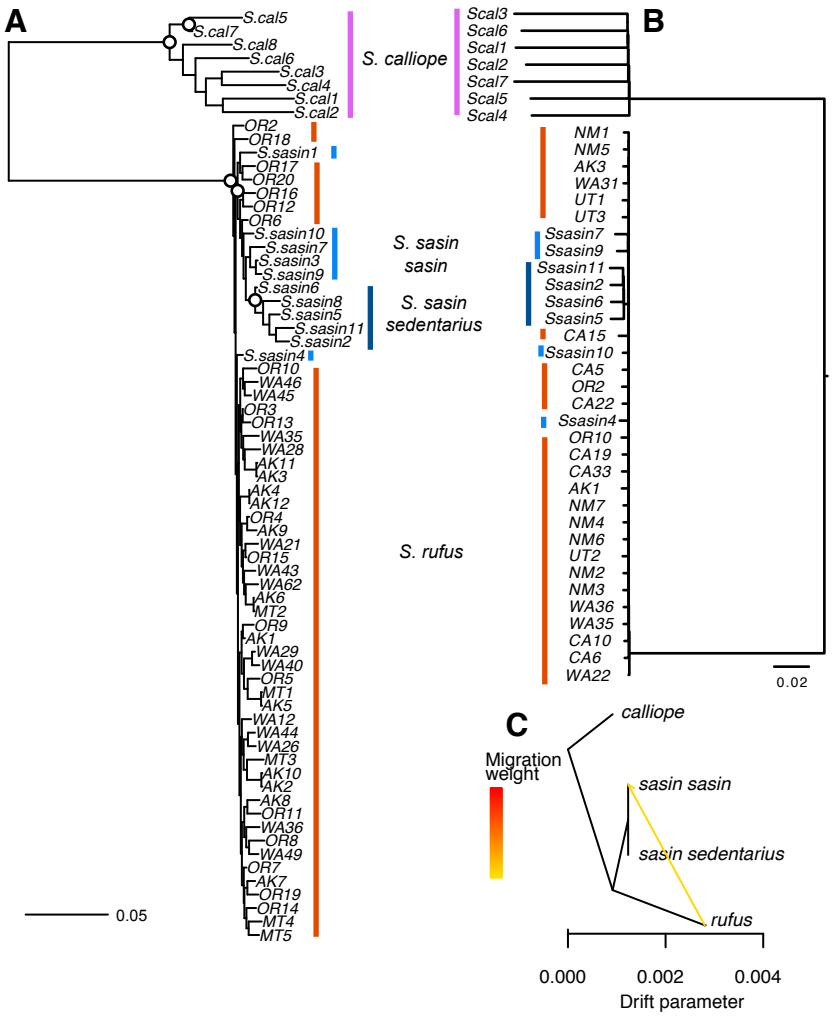

Figure 3.1: A: RAxML tree of concatenated ddRAD sequences from breeding individuals. Circles indicate nodes with over 90% bootstrap support. B: neighbor-joining tree of whole-genome SNP's. C: treemix population tree with one admixture edge.

3.3.4 Demographic Models

SMC++ (Terhorst et al., 2017) was used to estimate demographic histories from whole-genome sequence data. SMC++ implements a simple demographic model without migration between populations, but takes advantage of more of the information in whole-genome data than standard SFS based approaches like $\delta a \delta i$ by analyzing the distribution of variation across the genome rather than working from a single genome-wide estimate of the SFS. Because the whole genome data was unphased and we lack a detailed map of inaccessible regions of the *C. anna* reference genome, contiguous stretches of homozygosity greater than 30kbp were masked and inferences of population size in the last 2,000 years were dropped from smc++ runs. This reduces power to infer events in the recent past, but should minimize false signals of recent bottlenecks (Terhorst et al., 2017). I ran the all contigs $>$ 1 x 10^6bp, covering a total of 8.5 x 10^8bp, and constructed composite datasets using 4-8 different individuals as "designated individuals" (see Terhorst et al. 2017). Uncertainty in SMC++ analyses was estimated by creating bootstrapped datasets (sampling over contigs of the *C. anna* reference genome) and re-fitting models to 10 bootstrap replicates per population. I assumed

a mutation rate of 4.6e-9 substitutions/bp/generation and a generation time of one year, following a recent study based on deep sequencing of a pedigreed population of flycatchers (Smeds et al., 2016).

3.3.5 Introgression

The D statistic (Green et al., 2010) was used to test for introgression across all species, assuming a topology of (*calliope*,(*sasin*,*rufus*)). *D* was calculated for each combination of individuals conforming to the tree above using the "doAbbababba" function in ANGSD (6,019 comparisons total). Significance was assessed by block jacknife over 1mbp windows. Results were summarized by estimating the range of *D* values and associated bootstrap Z scores for each unique subspecies-level topology. A significant cutoff of Z = 4.31 was applied, equivalent to a p value of 0.05 after correcting for multiple comparisons.

3.3.6 Genome Scans

Within-population genetic diversity (π) and Tajima's D was calculated in 50,000bp non-overlapping windows for each species using the "doThetaStat" program in ANGSD. Pairwise relative divergence (*Fst*) was estimated with the "realSFS" program for three interspecific comparisons involving *S. rufus*: (1) *rufus* x *calliope*, (2) *rufus* x *sasin sedentarius*, and (3) *rufus* x *sasin sasin*; as well as for two intraspecific comparisons of populations showing behavioral or morphological variation: (4) *sasin sasin* x *sasin sedentarius* and (5) east x west migrating *rufus*. All of the above analyses were limited to only male samples (7 breeding *S. rufus*, 13 migrant *S. rufus*, 3 *S. calliope*, 4 *S. sasin sedentarius*, and 2 *S. sasin sasin*) to ensure that results were not biased by low coverage on the Z chromosome or incorrect alignment of variants from the W chromosome in females.

To estimate the position of *C. anna* contigs on avian chromosomes and facilitate comparisons with previous studies, each contig in the Korlach et al. 2017 *C. anna* genome was aligned to the most recent chromosome-scale assembly of the Zebra Finch (T̂aenopygia guttata; Warren et al. 2010) with the program 'MUMmer' (Delcher et al. 2003) and contigs were arranged by the start position of the longest matching stretch over 10,000 base pairs in the *T. guttata* genome. Contigs without matches in the *T. guttata* genome or with over 10,000bp of matching sequence to multiple chromosomes were binned into a separate "NA" category. Because the reference individual in Korlach et al. 2017 is a male, the W chromosome is not included in this analysis. All windowed analyses were conducted at the contig rather than the chromosome level.

The top 0.5% of windows for each summary statistic were identified as outliers for downstream analyses. Linear regression was used to test for correlations in *Fst* and *Dxy* across different taxonomic comparisons, and for per-window nucleotide diversity (π) across populations. After initial results suggested that differentiation was concentrated on the Z chromosome, I also estimated mean values of all statistics on the Z and the autosomes (excluding "NA" contigs).

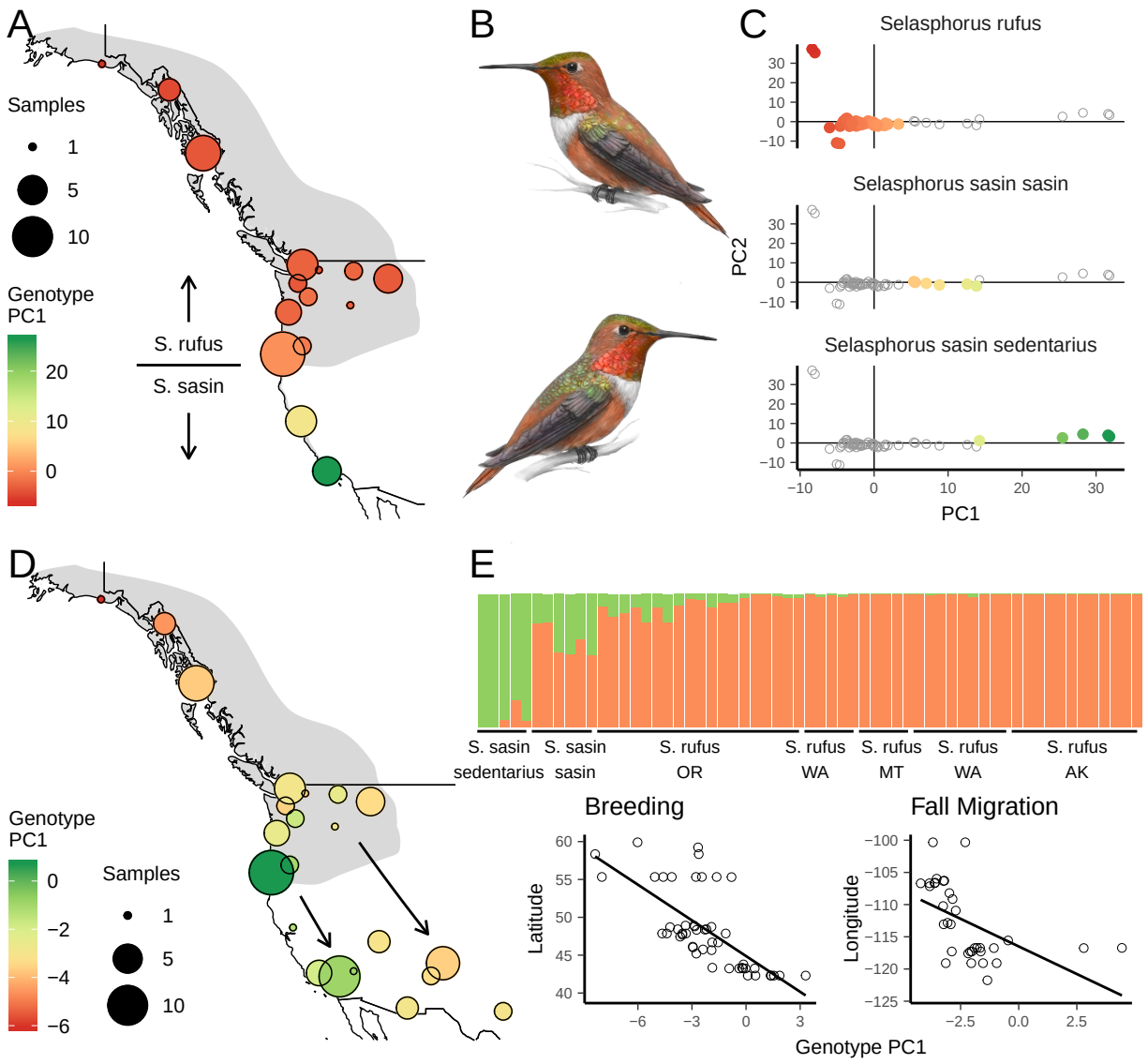

Figure 3.2: Population structure in *S. rufus* and *S. sasin*. A: Breeding season sampling sites scaled by number of samples and colored by mean genotype PC1. B: adult male *S. rufus* (top) and *S. sasin* (bottom; illustrations by Kevin Epperly). C: PCA on ddRAD genotypes of breeding samples. D: Population structure within *S. rufus* during breeding and migration. E: top-fitting *structure* results on breeding samples, sorted by latitude. F: correlations of *S. rufus* genotype PC1 with breeding latitude (left) and migration longitude (right).

3.4 Results

3.4.1 Phylogenetics and Population Structure

Phylogenetic and population tree inference on both concatenated ddRAD data and static whole-genome SNP calls found that *S. calliope* is sister to a combined clade of *S. rufus* and *S. sasin* (Figure 3.1), consistent with a recent study examining variation at six sanger-sequenced nuclear loci (Licona-Vera & Ornelas 2017). Though *S. calliope* is monophyletic, *S. rufus* and *S. sasin* form

a paraphyletic grade. Treemix also infers a migration edge from *S. rufus* to *S. sasin sasin*, consistent with their parapatric ranges and lack of monophyly in trees with individuals as tips.

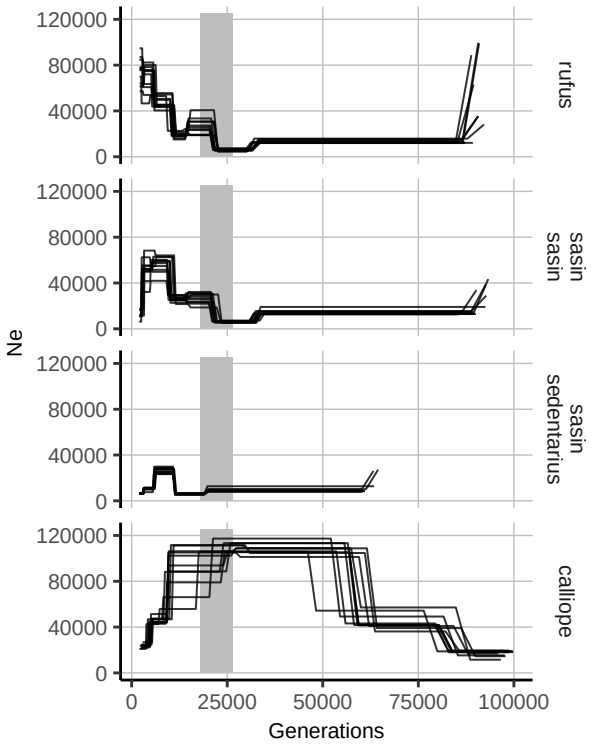

Figure 3.3: Estimates of population size histories from smc++. The grey bar indicates the timing of the LGM assuming a one-year generation time.

PCA's and Genotype clustering in *structure* both indicate that two-population models best describe the data, and suggest that most *S. sasin sasin* are admixed with *S. rufus* (Figure 3.2). *Structure* also infers 1-7% *S. sasin* ancestry in all breeding individuals from southern Oregon and 4 out of 16 migrants from California. However, the exact ancestry proportions in putative hybrids were highly sensitive to variation in sample size across runs so should be interpreted with some caution. In PC space the primary axis of differentiation is between *S. sasin sedentarius* and *S. rufus*, with *S. sasin sasin* and Oregon *S. rufus* falling in intermediate locations along PC1. Within *S. rufus*, both genotype PC1 and the fraction of inferred *S. sasin* ancestry in *structure* results decline with latitude (PC1: $p<0.01$, $R^2=0.48$). Across migrant populations of *S. rufus* PC1 is negatively correlated with longitude ($p=02$, $R^2=0.24$), suggesting that California migrants come primarily from southern and western areas of the breeding range while eastern migrants come from the rest of the range.

Mantel tests found that genetic and geographic distance were not correlated either across the full breeding range of *S. rufus* ($p=0.77$) or among migrants ($p=0.71$). However, genetic and geographic distance were correlated across breeding samples from Oregon and Washington ($p=0.017$), likely reflecting a consistent signal of *S. sasin* ancestry in Oregon birds.

3.4.2 Demography

Single-population demographic histories from smc++ inferred a population bottleneck between 20 and 30kya in *S. rufus* and *S. sasin sasin*, possibly reflecting the impacts of the last glacial maximum c. 18-26.5kya (Figure 3.3). Both *S. rufus* and *S. sasin* then grow to populations between 50,000 and 100,000 by 10kya, with *S. sasin* crashing after c. 3kya and *S. rufus* continuing to grow up to 2kya. *S. sasin sedentarius* is inferred to have experienced a small reduction in population size near the end of the LGM followed by a peak and then decline after 7kya. *S. calliope* grows to reach a peak population prior to the LGM and gradually declines after c. 20kya.

3.4.3 Introgression

D tests found evidence of significant introgression between *S. rufus* and *S. sasin* (Figure 3.4, Supplementary Table S1). Most introgression appears to be from *rufus* into *sasin*, because D scores were much higher for tests with two *sasin* in the P1/P2 positions. All combinations of individuals

tested on topologies with different subspecies of *S. sasin* in the P1/P2 positions returned significant results, reflecting a consistent pattern of excess *S. rufus* ancestry in *S. sasin sasin*.

Lower levels of introgression were also observed from *S. calliope* into both *S. sasin* and *S. rufus* (13-31% of tests), and from *S. sasin* into *S. rufus* (16-18% of tests). However these tests may simply reflect high levels of introgression between *rufus* and *sasin*. For example, when testing the topology ((*sasin*, *sasin*),*calliope*), some *sasin* may have received ancestral alleles shared with *S. calliope* as a result of gene flow from *rufus* and consequently have an unusually high number of discordant sites. The lack of any significant gene flow into *calliope* supports this hypothesis, though it could also be interpreted as evidence of unidirectional gene flow.

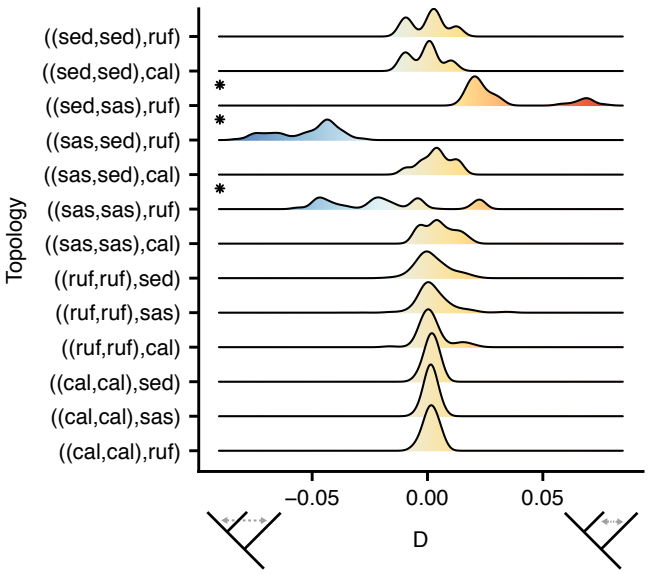

Figure 3.4: Distribution of D scores for "ABBA-BABA" introgression tests. Toplogies are listed as ((P1,P2),P3), with abbreviations cal=*calliope*, ruf=*rufus*, sas=*sasin sasin*, and sed=*sasin sedentarius*. Low D values reflect introgression between P1 and P3, and high values between P2 and P3. Asterisks indicate topologies with a median Z score over 3.1 (p<0.01 after correcting for 13 comparisons).

3.4.4 Genome Scans

Regions with the highest relative differentiation (*Fst*) in interspecific comparisons across northern *Selasphorus* are concentrated on the Z chromosome, but these regions have much lower than average within-population diversity (π) (Figure 3.5). *Fst* is not elevated in either comparisons of the two *S. sasin* subspecies, or between east and west-migrating *S. rufus*. Tajima's D is lower on the Z chromosome than the autosomes in all species (Figure 3.6, Supplementary Figure S2), with the largest relative differences in *S. rufus* and *S. sasin sedentarius*.

Within-population diversity (π) across all species is low but within the range observed in a recent review of avian genomic datasets (Table 3.3; (Irwin, 2018)). Per-window nucleotide diversity is strongly correlated in all comparisons of *rufus* and *sasin* (R^2=0.82-0.89) and moderately correlated in comparisons with *S. calliope* (R^2=0.44-0.47; Figure 3.6). In *rufus* and *sasin*, peaks of within population diversity also occur near the end of macrochromosomes (Figure 3.5). The ratio of autosomal to Z-linked π ranges from 0.44 to 0.55 across species – lower than the 0.75 ratio predicted by population size effects alone. *Fst* is weakly correlated across population pairs including *rufus* and *sasin* (R^2=0.04 - 0.29) but uncorrelated between east x west *rufus* and all other population pairs (Supplementary Figure S1).

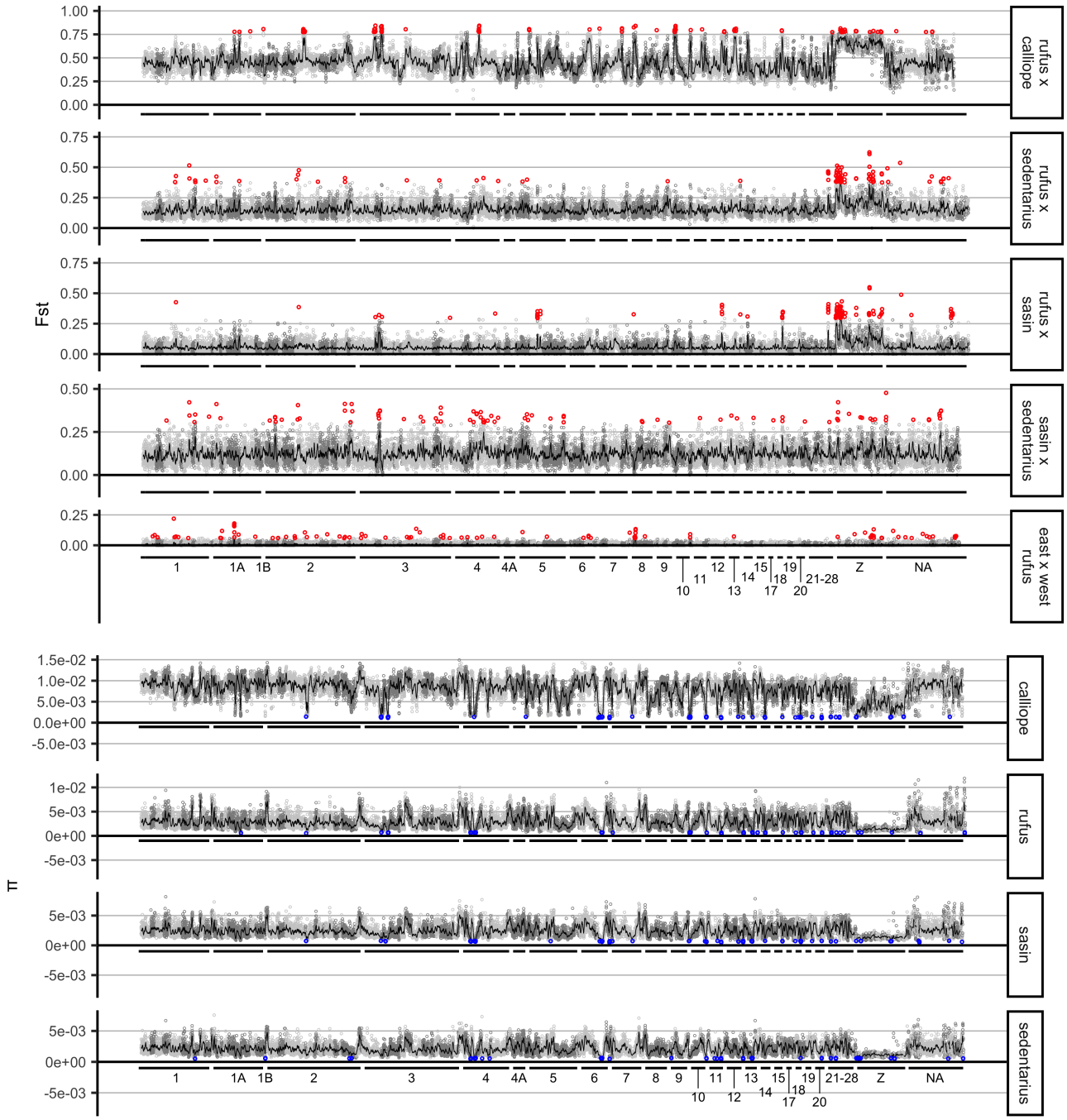

Figure 3.5: Relative divergence (*Fst*) and within-population diversity (π) in 50,000bp nonoverlapping windows. Red and blue circles are the top and bottom 0.5% of windows, the black line is a 1e6bp rolling average, and grey banding shows contigs of the Korlach et al. 2017 *C. anna* genome assembly. Contigs are ordered by their position in the *T. guttata* genome.

Species	π_a	π_z	π_z/π_a
calliope	0.00857	0.00380	0.44400
rufus	0.00266	0.00136	0.50900
sasin sasin	0.00230	0.00133	0.57900
sasin sedentarius	0.00197	0.00108	0.54700

Table 3.1: Mean within–population diversity on autosomes (π_a) and the Z-chromosome (π_z), by species.

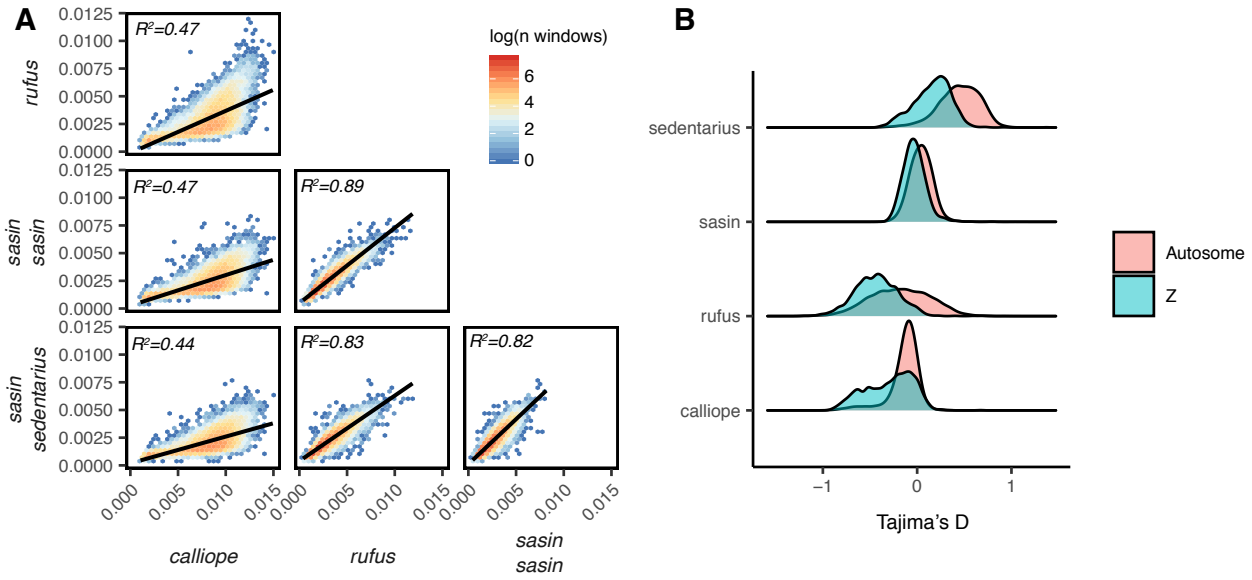

Figure 3.6: A: Correlation of nucleotide diversity (π) by genomic window. B: Distribution of Tajima's D on autosomes and the Z chromosome.

3.5 Discussion

3.5.1 Phylogeography

S. rufus and *S. sasin* diverged from *S. calliope* during the early Pleistocene and from each other in the late Pleistocene. Introgression and clustering analyses indicate that *rufus* and *sasin* have continued to experience gene flow after their divergence. Whole-genome demographic analyses infer a population bottleneck in both species at approximately 25,000 years in the past, possible reflecting the impacts of the last glacial maximum from 26 - 18kya. Both migratory populations then increase in population, which is consistent with an increase in available habitat in the Pacific Northwest after glacial retreat. Together these observations suggest that climate cycling in the late Pleistocene played a major role in lineage diversification in the group.

For *S. rufus*, most of the modern breeding range was either glaciated (all of the Puget Sound lowlands and most high-altitude regions of the Pacific Northwest) or was characterized by a much drier, colder climate than modern times until glacial retreat beginning around 18ya (Hovan et al., 1991). The expansion in suitable habitats as the climate of the Pacific Northwest became warmer and wetter likely contributed to increasing populations of this species, which is reflected in estimates of rising populations after c. 20kya in single-population demographic models. Glacial retreat also

corresponded with a significant drying and warming of the climate in California after 26 kya and a large rise in sea levels after 15kya (Herbert et al., 2001). In coastal California, sea level rise after the LGM shrunk the size of the coastal plane and decreased the land area of the Channel Islands by nearly 20%, with the most rapid change in land area occurring c. 3.5-5kya (Kinlan et al., 2005). Demographic models of *S. sasin sedentarius* indicate that effective population size has decreased over time, which may reflect the impacts of these biogeographic processes.

The migratory *S. sasin sasin* appears to be a hybrid taxon, including ancestry from both *S. rufus* and *S. sasin*. The subspecies likely diverged from *S. sasin sedentarius* during or after the onset of glacial retreat and subsequently began hybridizing with *S. rufus*, to the extent that much of the genome outside the Z chromosome of *S. sasin sasin* is more similar to *S. rufus* than to *S. sasin sedentarius* (Figure 3.5).

3.5.2 Migratory Connectivity in *S. rufus*

S. rufus makes the longest migratory journey of any hummingbird, covering up to 7,000 kilometers a year between Alaska and central Mexico. Like most migrants in the western US the species makes a clockwise loop around the continent, traveling up the Pacific Coast in spring and down the interior mountain ranges in fall. However, neither journey can be completed without refueling along the way. *S. rufus* heavily utilize mid-summer wildflower blooms in the Sierra Nevada and Rocky Mountains during their southbound fall migration (Hixon et al., 1983). Individuals can more than double their body mass over the course of a two-week stopover (Carpenter et al., 1993), and recent studies of museum specimens suggest that birds migrating through California and Arizona use this time to complete a prealternate molt (Sieburth and Pyle, 2018). Locating suitable stopover habitat is thus likely to be an important factor in individual survival and has the potential to shape patterns of gene flow across populations.

In songbirds, captive breeding studies have demonstrated that both the timing (Pulido et al., 2001) and direction (Helbig, 1991) of seasonal migration are strongly heritable. Heritable programming of migratory behavior has clear fitness benefits in these species, which (like hummingbirds) migrate individually and without guidance from parents. Though no study has examined the heritability or genetics of migratory behaviors in hummingbirds, the fitness implications are similar to songbirds – some level of pre-programmed timing and orientation should enable individuals to travel at the appropriate direction and time to locate suitable stopover sites and thus increase survival.

Here I found that the basic population structure of *S. rufus* is maintained through migration, as the north-south cline in *S. sasin* ancestry is flipped to an east-west cline during the southbound migration. Most migrants in the Rockies breed in the northern and eastern areas of the breeding range, while most migrants in the Sierra Nevada breed in Oregon and southern Washington. Assortative mating across breeding populations may increase fitness during migration by passing on combinations of alleles that direct juveniles either west to the Sierra Nevada or east to the Rockies while avoiding the relatively poor stopover habitats of the Columbia Plateau and Great Basin. However, the differentiation I observed across migratory populations is not as distinct as that found in species such as Swainson's Thrush (*Catharus ustulatus*; (Delmore and Irwin, 2014)) or Painted Buntings (. *Passerina ciris*, (Battey et al., 2018)), possibly because *S. rufus* is a much younger species than either of these taxa, which diverged from their closest ancestors in the early Pleistocene and likely maintained structured populations through multiple glacial cycles.

3.5.3 Linked Selection and Sex Chromosome Differentiation

Relative divergence across species of northern *Selasphorus* is concentrated on the Z chromosome, but this region has very low within-population diversity and relatively lower Tajima's D than the autosomes (Figure 3.6). Some of this pattern is due to increased drift on sex chromosomes caused by their low population size. Population size effects are further increased if sexual selection increases variance in male relative to female reproductive success. *Selasphorus* hummingbirds are lekking species in which males conduct display flights and "sing" for females by generating noise through vibration of tail and wing feathers during dives (Clark, 2014), suggesting that there is sexual selection on male reproductive traits in the group. Variance in male reproductive success is thus likely higher than among females, further reducing the effective population size of the Z chromosome because 2/3 of all copies in a given generation are carried by males.

Theoretical explorations of the impacts of hemizygosity and increased variance in reproductive success across sexes suggests that these processes can cumulatively lead to a Z:autosome *Ne* ratio of roughly 0.56 (Charlesworth, 2001). The ratios observed here range from 0.44 in *S. calliope* to 0.54 in *S. sasin*, suggesting that variance in reproductive success (i.e. female-biased sex ratios) can explain the drop in diversity in *S. sasin*, but is unlikely to explain all of the decreased diversity in *S. rufus* or *S. calliope*. This hypothesis is consistent with patterns observed in Tajima's D, which is particularly low on the Z chromosome in *S. rufus* and *S. sasin*. Although the complex demographic history of this group makes interpretation of Tajima's D difficult, negative values are expected after a recent selective sweep.

Across all species pairs nucleotide diversity in different regions of the genome is strongly correlated, suggesting that a conserved recombination landscape (Singhal et al., 2015) and other structural genomic features including variation in mutation rate or GC content leads to recurrent evolution of similar patterns of genetic variation across the genome during the early stages of divergence. This interpretation is also supported by the strong correlation in π across all population pairs (Figure 3.6). Genome-wide *Fst*, however, is strongly correlated only across comparisons of *S. rufus* and either *S. sasin* subspecies – likely reflecting introgression across the autosomes between *S. rufus* and *S. sasin sasin*. This suggests that though the Z chromosome is a consistent outlier, relative divergence of populations in most of the nuclear genome is driven primarily by drift during early divergence.

Linked selection acting on the Z chromosome could take the form of purifying selection removing deleterious variants that arose after lineage divergence, or could represent disruptive selection across species pairs, possibly in loci linked to plumage or display behaviors used in mate selection. Though I did not attempt to identify specific variants or genes under selection in this study, it is notable that males are much more morphologically differentiated than females across all species studied here – to the degree that females and juveniles often cannot be distinguished in the field. A plausible explanation for this pattern is that alleles on the Z are under disruptive selection between *S. sasin sasin* and *S. rufus*, and that this process causes most of the elevated differentiation and low diversity observed on the Z.

3.5.4 Systematics

S. rufus and *S. sasin* are often indistinguishable in the field, appear to hybridize frequently, and diverged much more recently than any other pair of Hummingbird species in North America (McGuire et al., 2014; Licona-Vera and Ornelas, 2017). Further, all *S. sasin sasin* ddRAD samples were inferred to have the majority of their ancestry from *S. rufus* despite being caught at least 500 kilometers south of the range boundary, and autosomal *Fst* is lower between *S. rufus* and *S. sasin sasin*

than between the two subspecies of *S. sasin*. Are they really different species, and if so, should *S. sasin sasin* be seen as the migratory subspecies of Allen's Hummingbird or the southernmost population of Rufous Hummingbird?

Under strict versions of biological (Mayr, 1948) or phylogenetic (Donoghue, 1985; Baum and Shaw, 1995) species criteria, *S. rufus* and *S. sasin* are not species because they interbreed and are not reciprocally monophyletic over the vast majority of the genome. Under the criteria used by the US Fish and Wildlife Service when delimiting Distinct Population Segments as "species" for the purposes of the Endangered Species Act (Waples and Gaggiotti, 2006), which emphasizes demographic independence and behavioral or morphological differentiation, they are certainly species. As with most cases of divergence with gene flow, whether or not we recognize populations as species depends on the criteria we use rather than the underlying concept of populations differentiating over time, and reasonable arguments can be made advocating for the recognition of "species" at any stage of divergence (De Queiroz, 2007).

More concretely, this analysis suggests that *S. rufus* and *S. sasin* as currently recognized are separate lineages displaying some degree of assortative mating and likely capable of responding to different selective regimes in the face of gene flow. First, assortative mating is reflected in the much greater divergence between Oregon *S. rufus* and the parapatric *S. sasin sasin* than is observed between any pair of breeding or migratory populations within *S. rufus*, and by the inference of at least two genotype clusters in *structure* results and PCA's. Second, breeding behaviors are reported to be consistently different between species (Healy and Calder, 2006), with *S. rufus* and *S. sasin* each performing characteristic flight patterns while displaying for females at leks. Investigations of this behavior in the likely hybrid zone in southern Oregon and northern California are ongoing (Bryan Meyers *pers comm*), and should lead to further insight into the strength of assortative mating.

Third, relative differentiation of the sex chromosomes is elevated between *rufus* and both *sasin* subspecies, but not within either species. The reduction in genetic diversity and Tajima's D on this chromosome suggests that it is under selection in both species, and the elevated differentiation (relative to autosomes) in interspecific but not intraspecific comparisons suggests that the Z chromosome specifically is resistant to gene flow across species. Similar to cases of Blue and Golden-Winged Warblers (Toews et al., 2016) and Ficedula flycatchers (Saether et al., 2007), loci associated with sexually selected plumage or behavioral traits may be concentrated on the Z in *Selasphorus* hummingbirds, and elevated relative differentiation may reflect disruptive selection and indicate that combinations of traits important in reproductive isolation are maintained in different species. Whether this level of differentiation and selective coherence will eventually lead to reproductive isolation is unknown, but at present these populations appear to be evolving on separate evolutionary trajectories.

3.6 Conclusion

S. rufus and *S. sasin* diverged in the late Pleistocene and subsequently experienced different demographic histories, with both migratory populations increasing in population and hybridizing in northern California and southern Oregon while sedentary birds on the Channel Islands and southern California coast maintained low populations through the Holocene. Relative genetic differentiation across northern *Selasphorus* is concentrated on the Z chromosome, which is also the least diverse region of the genome in all species. The drop in diversity observed on the Z chromosome is greater than that expected from population size and mutation rate effects alone, suggesting that increased variance in male reproductive success and linked selection explains much of the reduction in diversity. Though within-population diversity is strongly correlated across species, relative divergence

(*Fst*) is weakly correlated in different taxonomic comparisons. Together these results suggest that linked selection is a prominent driver of variation in genetic differentiation across the genome of northern *Selasphorus* hummingbirds, and that the Z chromosome is a likely site of genes underlying behavioral and morphological variation in the group.

3.7 Data

Sample data including catalogue numbers of sequenced specimens :
https://www.dropbox.com/sh/61pgeye42jmhh1b/AACb7rN6HWwoB2BcpKmA9gfha?dl=0

3.8 Acknowledgements

Tissue samples analyzed in this study were contributed by the Burke Museum of Natural History, Louisiana State University Museum of Natural Sciences, University of New Mexico Museum of Southwestern Biology, University of California Berkeley Museum of Vertebrate Zoology, and University of Alaska Museum of the North. Ethan Linck and Adam Leaché provided helpful comments on earlier versions of this manuscript. Members of Klicka Lab at the University of Washington from 2013 - 2018 all contributed to the development and refinement of ideas and analyses presented here. Thanks to Ethan Linck, Cooper French, Dave Slager, John Klicka, and Rob Bryson. This project was supported by grants from the University of Washington Dept. of Biology and NSF grant # DEB1600945.

3.9 Supplementary Figures and Tables

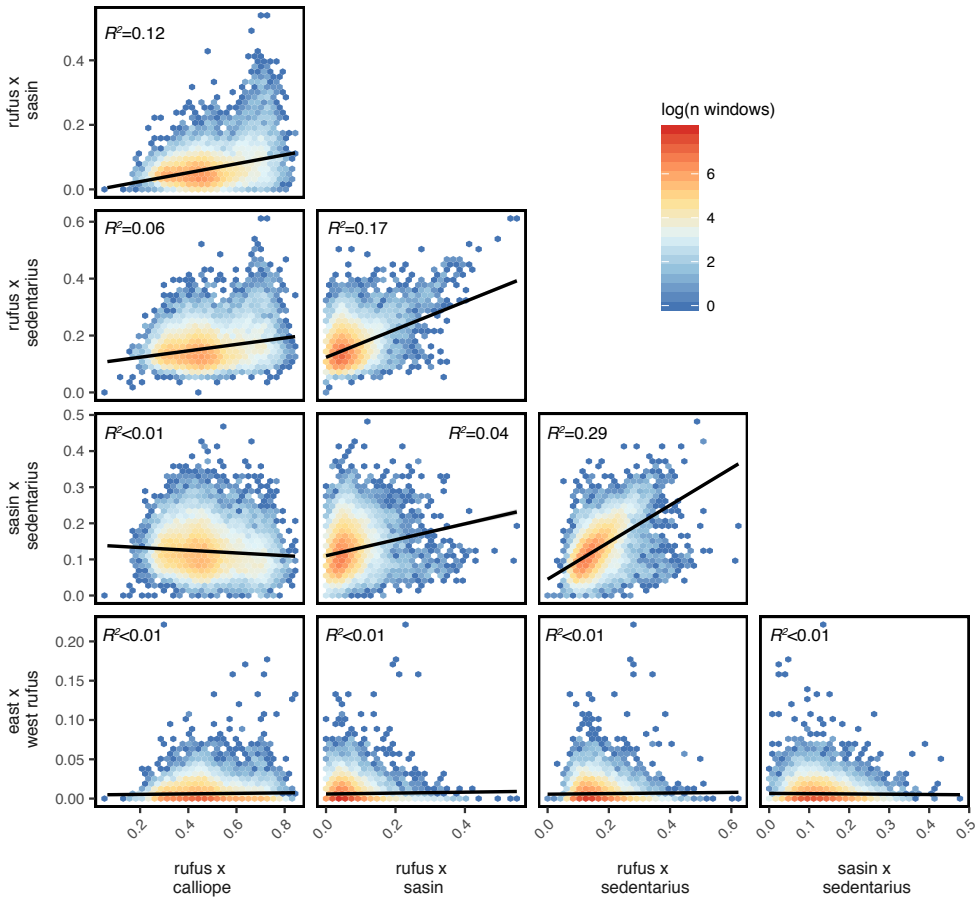

Figure S1: Correlation of relative divergence (Fst) by genomic window across population pairs.

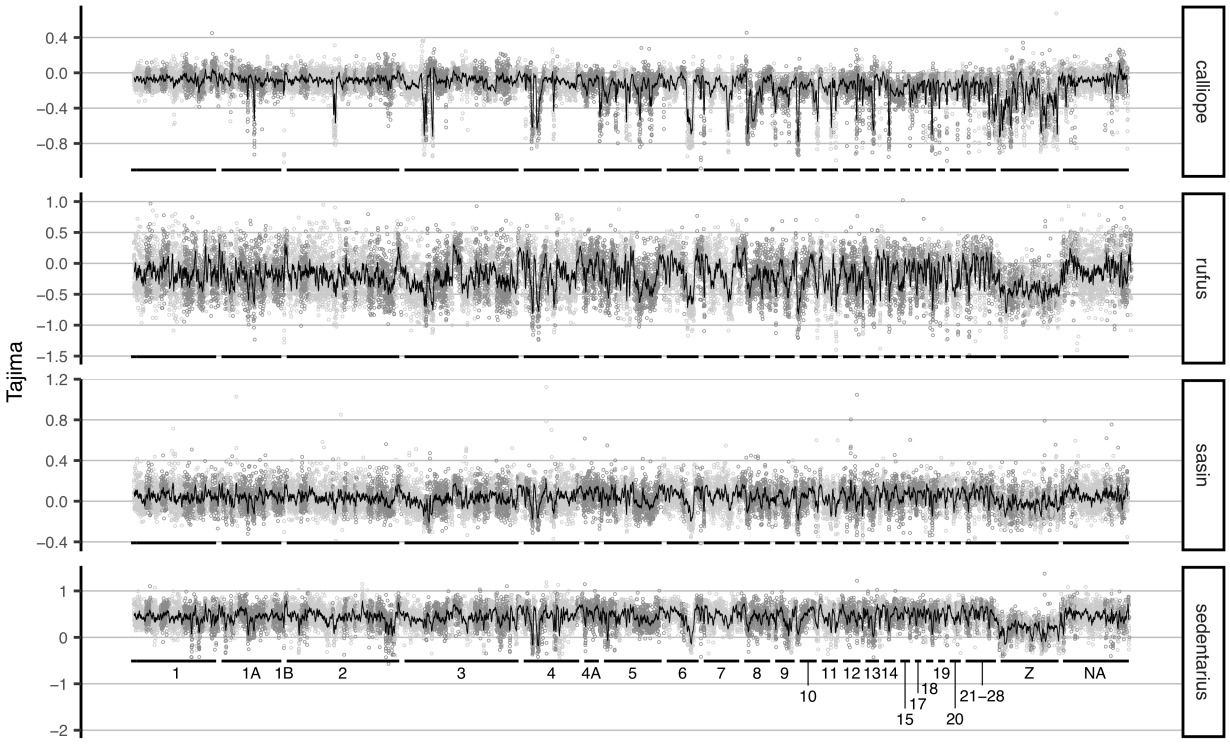

Figure S2: Tajima's D in 50,000bp nonoverlapping windows.

Topology	nABBA	nBABA	median(D)	median(Z)	Proportion Significant
((cal,cal),ruf)	888992	887517	1.55e-03	1.60	0.01
((cal,cal),sas)	888044	883494	1.46e-03	1.37	0
((cal,cal),sed)	807972	804756	1.72e-03	1.59	0
((ruf,ruf),cal)	240352	239622	9.38e-04	1.30	0.13
((ruf,ruf),sas)	416843	415232	1.4e-03	1.84	0.16
((ruf,ruf),sed)	366410	365356	9.16e-04	2.12	0.18
((sas,sas),cal)	252702	250484	3.82e-03	2.76	0.21
((sas,sas),ruf)	434201	447260	-2.11e-02	9.85	0.82
((sas,sed),cal)	235619	234969	3.89e-03	2.28	0.24
((sas,sed),ruf)	386812	435396	-4.68e-02	18.30	1
((sed,sas),ruf)	396048	374092	2.26e-02	11.70	1
((sed,sed),cal)	163162	164162	3.11e-04	1.99	0.31
((sed,sed),ruf)	274520	277976	1.44e-03	2.94	0.38

Table S1: Summary of D test results. D values and counts of ABBA and BABA sites are medians; Z scores are median absolute values. Proportion significant is the proportion of all individual combinations under a given topology with a abs(Z) $>$ 4.3.

SampleID	*Selasphorus* sp.	Museum	Prep Number	Museum Number	State	Latitude	Longitude
AK1	*rufus*	UAM	RWD24097	7468	AK	55.312	-131.570
AK10	*rufus*	UAM	ABJ651	15394	AK	55.331	-131.619
AK11	*rufus*	UAM	UAMX178	9977	AK	55.331	-131.619
AK12	*rufus*	UAM	ABJ103	13100	AK	55.331	-131.619
AK2	*rufus*	UAM	JJW1573	30194	AK	59.904	-141.326
AK3	*rufus*	UAM	RWD24014	7469	AK	58.3449	-134.555
AK4	*rufus*	UAM	UAMX2175	13891	AK	55.331	-131.619
AK5	*rufus*	UAM	UAMX2174	13896	AK	55.331	-131.619
AK6	*rufus*	UAM	UAMX2173	13895	AK	55.331	-131.619
AK7	*rufus*	UAM	UAMX4263	22246	AK	59.232	-135.4642
AK8	*rufus*	UAM	JJW877	27373	AK	58.344	-134.555
AK9	*rufus*	UAM	JJW1158	20383	AK	55.331	-131.619
AZ1	*rufus*	UWBM	RBB794	87082	AZ	32.222	-110.926
AZ2	*rufus*	UWBM	CEC500	119790	AZ	31.380	-110.228
CA1	*rufus*	UWBM	RBB479	86827	CA	38.535	-121.754
CA10	*rufus*	LSU	SWC7652	B-30336	CA	34.820	-119.097
CA11	*rufus*	LSU	SWC7653	B-30337	CA	34.820	-119.097
CA12	*rufus*	LSU	DLD6758	B-30514	CA	34.172	-116.725
CA13	*rufus*	LSU	EAC7798	B-41970	CA	34.172	-116.725
CA14	*rufus*	LSU	EAC7823	B-41998	CA	34.172	-116.725
CA15	*rufus*	LSU	EAC9383	B-51775	CA	34.223	-116.750
CA16	*rufus*	LSU	EAC9412	B-51804	CA	34.223	-116.750
CA17	*rufus*	LSU	EAC9413	B-51805	CA	34.223	-116.750
CA2	*rufus*	LSU	EAC3105	B-19499	CA	35.008	-117.284
CA3	*rufus*	LSU		B-19500	CA	35.009	-117.284
CA4	*rufus*	LSU	EAC310?	B-19514	CA	35.008	-117.284
CA5	*rufus*	LSU	EAC3108	B-19515	CA	35.008	-117.284
CA6	*rufus*	LSU	EAC7470	B-24253	CA	34.602	-117.579
CA7	*rufus*	LSU	DLD4794	B-25054	CA	34.971	-115.571
CA8	*rufus*	LSU	SWC7647	B-30331	CA	34.819	-119.097
CA9	*rufus*	LSU	SWC7651	B-30335	CA	34.819	-119.097
MT1	*rufus*	UWBM	CJB081	pending	MT	47.862	-113.841
MT2	*rufus*	UWBM	CJB082	pending	MT	47.862	-113.841
MT3	*rufus*	UWBM	CJB083	pending	MT	47.862	-113.841
MT4	*rufus*	UWBM	CJB085	pending	MT	47.862	-113.841
MT5	*rufus*	UWBM	CJB087	pending	MT	47.862	-113.841

Table S2: ddRAD specimen information - part 1.

SampleID	*Selasphorus* sp.	Museum	Prep Number	Museum Number	State	Latitude	Longitude
NM1	*rufus*	MSB	116031	23795	NM	35.768	-106.692
NM10	*rufus*	MSB	221743	40230	NM	31.91	-109.14
NM2	*rufus*	MSB	142268	25453	NM	35.875	-106.328
NM3	*rufus*	MSB	169609	26896	NM	35.151	-108.211
NM4	*rufus*	MSB	170948	29562	NM	35.889	-106.287
NM5	*rufus*	MSB	170952	29566	NM	35.89	-105.98
NM6	*rufus*	MSB	173138	29844	NM	33.993	-107.144
NM7	*rufus*	MSB	174757	30838	NM	35.77	-106.69
NM8	*rufus*	MSB	174808	30908	NM	35.090	-106.592
NM9	*rufus*	MSB	218283	39413	NM	35.13	-106.68
OR1	*rufus*	UWBM	TNL183	91462	OR	44.0537	-121.313
OR10	*rufus*	UWBM	CSW6067	64429	OR	43.345	-122.091
OR11	*rufus*	UWBM	CEC685	120043	OR	46.024	-123.911
OR12	*rufus*	UWBM	BTS06279	100539	OR	42.303	-123.781
OR13	*rufus*	UWBM	BTS06275	100534	OR	43.245	-124.12
OR14	*rufus*	UWBM	BTS06280	100540	OR	42.304	-123.781
OR15	*rufus*	UWBM	BTS06281	100541	OR	43.245	-124.12
OR16	*rufus*	UWBM	BTS06282	100542	OR	42.303	-123.781
OR17	*rufus*	UWBM	BTS06286	100546	OR	42.303	-123.781
OR18	*rufus*	UWBM	CJB088	pending	OR	43.245	-124.045
OR19	*rufus*	UWBM	CJB089	pending	OR	42.303	-123 46.9
OR2	*rufus*	UWBM	SMB101	64552	OR	43.345	-122.09
OR20	*rufus*	UWBM	CJB090	pending	OR	42.303	-123 46.9
OR3	*rufus*	UWBM	JK06 824	112781	OR	43.78	-124.015
OR4	*rufus*	UWBM	GKD595	79617	OR	45.659	-122.863
OR5	*rufus*	UWBM	GHL034	86050	OR	45.758	-122.88
OR6	*rufus*	UWBM	BTS06277	100537	OR	42.304	-123.781
OR7	*rufus*	UWBM	BTS06278	100538	OR	43.245	-124.12
OR8	*rufus*	UWBM	BTS06276	100535	OR	43.245	-124.12
OR9	*rufus*	UWBM	CEC686	119823	OR	45.2023	-123.9629
S.cal1	*calliope*	UWBM	CSW7612	90538	WA		
S.cal2	*calliope*	UWBM	CEC602	119809	NM	35.082	-106.817
S.cal3	*calliope*	UWBM	CJB091	pending	WA	45.125	-116.479
S.cal4	*calliope*	MVZ		183560	CA	37.53286	-118.157
S.cal5	*calliope*	MVZ		182181	CA	40.565523	-120.756
S.cal6	*calliope*	MVZ		182180	CA	40.6661	-120.837
S.cal7	*calliope*	MVZ		182361	CA	40.34428	-121.433
S.cal8	*calliope*	MVZ		183708	CA	39.433192	-120.261

Table S3: ddRAD specimen information - part 2.

SampleID	*Selasphorus* sp.	Museum	Prep Number	Museum Number	State	Latitude	Longitude
S.sasin1	*sasin sasin*	UWBM	GSB 054	80061	CA	37.919	-122.696
S.sasin10	*sasin sasin*	MVZ		180045	CA	37.866	-122.152
S.sasin11	*sasin sedentarius*	MVZ		183552	CA	33.996	-119.725
S.sasin2	*sasin sedentarius*	MVZ		183554	CA	33.996	-119.725
S.sasin3	*sasin sasin*	MVZ		180487	CA	37.972	-122.012
S.sasin4	*sasin sasin*	MVZ		182025	CA	37.681	-121.756
S.sasin5	*sasin sedentarius*	MVZ		183549	CA	33.996	-119.725
S.sasin6	*sasin sedentarius*	MVZ		183551	CA	33.996	-119.725
S.sasin7	*sasin sasin*	MVZ		183714	CA	37.889	-122.319
S.sasin8	*sasin sedentarius*	MVZ		183550	CA	33.996	-119.725
S.sasin9	*sasin sasin*	MVZ		183713	CA	37.890	-122.318
TX1	*rufus*	LSU		B-91622	TX	31.550	-100.327
TX2	*rufus*	LSU		B-91623	TX	31.550	-100.327
UT1	*rufus*	UWBM	JK09 597	114234	UT	36.678	-113.0612
UT2	*rufus*	UWBM	JK04 576	111649	UT	37.678	-113.0612
UT3	*rufus*	UWBM	JK00 304	99309	UT	37.842	-112.828
WA12	*rufus*	UWBM		62641	WA	48.8	-121.92
WA21	*rufus*	UWBM		57305	WA	48.907	-121.659
WA26	*rufus*	UWBM		57307	WA	48.907	-121.659
WA27	*rufus*	UWBM		84224	WA	47.642	-122.542
WA28	*rufus*	UWBM		99531	WA	48.71	-122.442
WA29	*rufus*	UWBM		99530	WA	47.69	-122.565
WA35	*rufus*	UWBM		54064	WA	48.37	-117.19
WA36	*rufus*	UWBM		54058	WA	48.34	-117.14
WA40	*rufus*	UWBM		118223	WA	48.42	-120.503
WA43	*rufus*	UWBM		72972	WA	46.686	-121.523
WA44	*rufus*	UWBM		72973	WA	46.686	-121.523
WA45	*rufus*	UWBM		119827	WA	48.425	-122.288
WA46	*rufus*	UWBM		119658	WA	47.447	-122.459
WA49	*rufus*	UWBM		120045	WA	48.741	-122.474
WA62	*rufus*	UWBM	CJB092	pending	WA	48.34	-117.14

Table S4: ddRAD specimen information - part 3.

SampleID	*Selasphorus* sp.	Museum	Museum Number	Latitude	Longitude	Sex
WA35	*rufus*	UWBM	64429	43.35	-122.09	male
WA36	*rufus*	UWBM	64552	43.35	-122.09	male
OR2	*rufus*	UWBM	54058	48.34	-117.14	male
OR10	*rufus*	UWBM	54064	48.37	-117.19	male
WA22	*rufus*	UWBM	86002	47.69	-122.32	male
WA31	*rufus*	UWBM	86027	47.80	-122.66	male
AK1	*rufus*	UAM	7468	55.31	-131.57	female
AK3	*rufus*	UAM	7469	58.34	-134.56	male
S.sasin4	*sasin sasin*	MVZ	182025	37.68	-121.76	female
S.sasin7	*sasin sasin*	MVZ	183714	37.89	-122.32	male
S.sasin9	*sasin sasin*	MVZ	183713	37.89	-122.32	male
S.sasin10	*sasin sasin*	MVZ	180045	37.87	-122.15	female
S.sasin2	*sasin sedentarius*	MVZ	183554	34.00	-119.73	male
S.sasin5	*sasin sedentarius*	MVZ	183549	34.00	-119.73	male
S.sasin6	*sasin sedentarius*	MVZ	183551	34.00	-119.73	male
S.sasin11	*sasin sedentarius*	MVZ	183552	34.00	-119.73	male
S.cal1	*calliope*	UWBM	90538	47.01	-120.66	female
S.cal3	*calliope*	UWBM	pending	45.12	-116.48	female
S.cal5	*calliope*	MVZ	182181	40.57	-120.76	male
S.cal7	*calliope*	MVZ	182361	40.34	-121.43	female
UT1	*rufus*	UWBM	114234	36.68	-113.06	male
UT2	*rufus*	UWBM	111649	37.68	-113.06	male
UT3	*rufus*	UWBM	99309	37.84	-112.83	male
AZ1	*rufus*	UWBM	87082	32.22	-110.93	female
AZ2	*rufus*	UWBM	119790	31.38	-110.23	male
NM1	*rufus*	MSB	23795	35.77	-106.69	male
NM2	*rufus*	MSB	25453	35.88	-106.33	female
NM3	*rufus*	MSB	26896	35.15	-108.21	male
NM4	*rufus*	MSB	29562	35.89	-106.29	male
NM5	*rufus*	MSB	29566	35.89	-105.98	male
NM6	*rufus*	MSB	29844	33.99	-107.14	male
NM7	*rufus*	MSB	30838	35.77	-106.69	male
NM8	*rufus*	MSB	30908	35.09	-106.59	male
CA10	*rufus*	LSU	B-30336	34.82	-119.10	female
CA19	*rufus*	MVZ	182183	40.57	-120.76	male
CA21	*rufus*	MVZ	183710	39.43	-120.26	male
CA22	*rufus*	MVZ	183712	39.43	-120.26	male
CA5	*rufus*	LSU	B-19515	35.01	-117.28	male
CA6	*rufus*	LSU	B-24253	34.60	-117.58	male
CA33	*rufus*	MVZ	182363	40.37	-121.54	female
CA15	*rufus*	LSU	B-51775	34.22	-116.75	female
S.cal2	*calliope*	UWBM	119809	35.08	-106.82	male
S.cal4	*calliope*	MVZ	183560	37.53	-118.16	female
S.cal6	*calliope*	MVZ	182180	40.67	-120.84	male

Table S5: Whole-genome sequencing specimen data.

Bibliography

Hirotugu Akaike. Factor analysis and AIC. In *Selected Papers of Hirotugu Akaike*, pages 371–386. Springer, 1987.

Sonia Altizer and Andrew K Davis. Populations of monarch butterflies with different migratory behaviors show divergence in wing morphology. *Evolution*, 64(4):1018–1028, April 2010.

American Ornithologists' Union. *Check-list of North American Birds*. American Ornithologists' Union, 1910.

Nidia Arguedas and Patricia G Parker. SEASONAL MIGRATION AND GENETIC POPULATION STRUCTURE IN HOUSE WRENS. *Condor*, 102(3):517–528, August 2000.

C S Baker, R W Slade, J L Bannister, R B Abernethy, M T Weinrich, J Lien, J Urban, P Corkeron, J Calmabokidis, O Vasquez, and Others. Hierarchical structure of mitochondrial DNA gene flow among humpback whales megaptera novaeangliae, world-wide. *Mol. Ecol.*, 3(4):313–327, 1994.

B R Barber and J Klicka. Two pulses of diversification across the isthmus of tehuantepec in a montane mexican bird fauna. *Proc. Biol. Sci.*, 277(1694):2675–2681, September 2010.

C J Battey. cjbattey/structureplotter: structureplotter_v1, March 2017.

C J Battey, Ethan B Linck, Kevin L Epperly, Cooper French, David L Slager, Paul W Sykes, Jr, and John Klicka. A migratory divide in the painted bunting (passerina ciris). *Am. Nat.*, 191(2): 259–268, February 2018.

Christopher J Battey, Ethan B Linck, Kevin L Epperly, Cooper French, David L Slager, Paul W Sykes, Jr., and John Klicka. Data from: A migratory divide in the painted bunting (passerina ciris), September 2017.

David A Baum and Kerry L Shaw. Genealogical perspectives on the species problem. *Experimental and molecular approaches to plant biosystematics*, 53(289-303):123–124, 1995.

Stuart Bearhop, Wolfgang Fiedler, Robert W Furness, Stephen C Votier, Susan Waldron, Jason Newton, Gabriel J Bowen, Peter Berthold, and Keith Farnsworth. Assortative mating as a mechanism for rapid evolution of a migratory divide. *Science*, 310(5747):502–504, October 2005.

Richard A Becker, Allan R Wilks, Ray Brownrigg, and Thomas P Minka. maps: Draw geographical maps. *R package version*, 2, 2013.

Remco Bouckaert, Joseph Heled, Denise Kühnert, Tim Vaughan, Chieh-Hsi Wu, Dong Xie, Marc A Suchard, Andrew Rambaut, and Alexei J Drummond. BEAST 2: a software platform for bayesian evolutionary analysis. *PLoS Comput. Biol.*, 10(4):e1003537, April 2014.

David Bryant, Remco Bouckaert, Joseph Felsenstein, Noah A Rosenberg, and Arindam RoyChoudhury. Inferring species trees directly from biallelic genetic markers: bypassing gene trees in a full coalescent analysis. *Mol. Biol. Evol.*, 29(8):1917–1932, August 2012.

Kenneth P Burnham and David R Anderson. Multimodel inference: Understanding AIC and BIC in model selection. *Sociol. Methods Res.*, 33(2):261–304, November 2004.

Steven X Cadrin, Lisa A Karr, and Stefano Mariani. Stock identification methods: an overview. In *Stock Identification Methods (Second Edition)*, pages 1–5. Elsevier, 2014.

F Lynn Carpenter, Mark A Hixon, Carol A Beuchat, Robert W Russell, and David C Paton. Biphasic mass gain in migrant hummingbirds: Body composition changes, torpor, and ecological significance. *Ecology*, 74(4):1173–1182, June 1993.

Julian Catchen, Paul A Hohenlohe, Susan Bassham, Angel Amores, and William A Cresko. Stacks: an analysis tool set for population genomics. *Mol. Ecol.*, 22(11):3124–3140, June 2013.

B Charlesworth. The effect of life-history and mode of inheritance on neutral genetic variability. *Genet. Res.*, 77(2):153–166, April 2001.

David A Cimprich, R R Morse, and Michael P Guilfoyle. Red-eyed Vireo(Vireo olivaceus). *Birds North America*, (527):24, 2000.

Christopher James Clark. Harmonic hopping, and both punctuated and gradual evolution of acoustic characters in selasphorus hummingbird tail-feathers. *PLoS One*, 9(4):e93829, April 2014.

Andrea Contina, Eli S Bridge, Nathaniel E Seavy, Jonah M Duckles, and Jeffrey F Kelly. Using geologgers to investigate bimodal isotope patterns in painted buntings (passerina ciris). *Auk*, 130 (2):265–272, April 2013.

Brandon S Cooper, Alisa Sedghifar, W Thurston Nash, Aaron A Comeault, and Daniel R Matute. A maladaptive combination of traits contributes to the maintenance of a drosophila hybrid zone. *Curr. Biol.*, 0(0), August 2018.

J A Coyne and T D Price. Little evidence for sympatric speciation in island birds. *Evolution*, 54 (6):2166–2171, December 2000.

Tami E Cruickshank and Matthew W Hahn. Reanalysis suggests that genomic islands of speciation are due to reduced diversity, not reduced gene flow. *Mol. Ecol.*, 23(13):3133–3157, July 2014.

Jeffrey M DaCosta and Michael D Sorenson. ddRAD-seq phylogenetics based on nucleotide, indel, and presence-absence polymorphisms: Analyses of two avian genera with contrasting histories. *Mol. Phylogenet. Evol.*, 94(Pt A):122–135, January 2016.

Petr Danecek, Adam Auton, Goncalo Abecasis, Cornelis A Albers, Eric Banks, Mark A DePristo, Robert E Handsaker, Gerton Lunter, Gabor T Marth, Stephen T Sherry, Gilean McVean, Richard Durbin, and 1000 Genomes Project Analysis Group. The variant call format and VCFtools. *Bioinformatics*, 27(15):2156–2158, August 2011.

Kevin De Queiroz. Species concepts and species delimitation. *Syst. Biol.*, 56(6):879–886, December 2007.

Kira E Delmore and Darren E Irwin. Hybrid songbirds employ intermediate routes in a migratory divide. *Ecol. Lett.*, 17(10):1211–1218, October 2014.

Kira E Delmore, Juan S Lugo Ramos, Benjamin M Van Doren, Max Lundberg, Staffan Bensch, Darren E Irwin, and Miriam Liedvogel. Comparative analysis examining patterns of genomic differentiation across multiple episodes of population divergence in birds. *Evolution Letters*, 2(2): 76–87, April 2018.

Michael J Donoghue. A critique of the biological species concept and recommendations for a phylogenetic alternative. *Bryologist*, pages 172–181, 1985.

Dent A Earl and Bridgett M vonHoldt. STRUCTURE HARVESTER: a website and program for visualizing STRUCTURE output and implementing the evanno method. *Conserv. Genet. Resour.*, 4(2):359–361, June 2012.

Deren A R Eaton. PyRAD: assembly of de novo RADseq loci for phylogenetic analyses. *Bioinformatics*, 30(13):1844–1849, July 2014.

Deren A R Eaton and Richard H Ree. Inferring phylogeny and introgression using RADseq data: an example from flowering plants (pedicularis: Orobanchaceae). *Syst. Biol.*, 62(5):689–706, September 2013.

Deren A R Eaton, Andrew L Hipp, Antonio González-Rodríguez, and Jeannine Cavender-Bares. Historical introgression among the american live oaks and the comparative nature of tests for introgression. *Evolution*, 69(10):2587–2601, October 2015.

Robert C Edgar. MUSCLE: multiple sequence alignment with high accuracy and high throughput. *Nucleic Acids Res.*, 32(5):1792–1797, March 2004.

Robert C Edgar. Search and clustering orders of magnitude faster than BLAST. *Bioinformatics*, 26(19):2460–2461, October 2010.

G Evanno, S Regnaut, and J Goudet. Detecting the number of clusters of individuals using the software STRUCTURE: a simulation study. *Mol. Ecol.*, 14(8):2611–2620, July 2005.

L Excoffier, P E Smouse, and J M Quattro. Analysis of molecular variance inferred from metric distances among DNA haplotypes: application to human mitochondrial DNA restriction data. *Genetics*, 131(2):479–491, June 1992.

Laurent Georges Louis Excoffier. Analysis of population subdivision. 2001.

John Faaborg, Richard T Holmes, Angela D Anders, Keith L Bildstein, Katie M Dugger, Sidney A Gauthreaux, Jr, Patricia Heglund, Keith A Hobson, Alex E Jahn, Douglas H Johnson, Steven C Latta, Douglas J Levey, Peter P Marra, Christopher L Merkord, Erica Nol, Stephen I Rothstein, Thomas W Sherry, T Scott Sillett, Frank R Thompson, III, and Nils Warnock. Recent advances in understanding migration systems of new world land birds. *Ecol. Monogr.*, 80(1):3–48, February 2010.

Daniel Falush, Matthew Stephens, and Jonathan K Pritchard. Inference of population structure using multilocus genotype data: linked loci and correlated allele frequencies. *Genetics*, 164(4): 1567–1587, August 2003.

Daniel Falush, Lucy van Dorp, and Daniel Lawson. A tutorial on how (not) to over-interpret STRUCTURE/ADMIXTURE bar plots. July 2016.

U S Fish, Wildlife Service, and Others. *Birds of conservation concern 2002*. US Fish and Wildlife Service, 2002.

Michael C Fontaine, James B Pease, Aaron Steele, Robert M Waterhouse, Daniel E Neafsey, Igor V Sharakhov, Xiaofang Jiang, Andrew B Hall, Flaminia Catteruccia, Evdoxia Kakani, Sara N Mitchell, Yi-Chieh Wu, Hilary A Smith, R Rebecca Love, Mara K Lawniczak, Michel A Slotman, Scott J Emrich, Matthew W Hahn, and Nora J Besansky. Mosquito genomics. extensive introgression in a malaria vector species complex revealed by phylogenomics. *Science*, 347(6217): 1258524, January 2015.

A M Frazar. Destruction of birds by a storm while migrating. *Bulletin of the Nuttall Ornithological Club*, 6(4):250–252, 1881.

Belen Garcia-Perez, Keith A Hobson, Rebecca L Powell, Christopher J Still, and Gernot H Huber. Switching hemispheres: a new migration strategy for the disjunct argentinean breeding population of barn swallow (hirundo rustica). *PLoS One*, 8(1):e55654, January 2013.

Bronwyn M Gillanders. Temporal and spatial variability in elemental composition of otoliths: implications for determining stock identity and connectivity of populations. *Can. J. Fish. Aquat. Sci.*, 59(4):669–679, April 2002.

Jeffrey M Good, Dan Vanderpool, Sara Keeble, and Ke Bi. Negligible nuclear introgression despite complete mitochondrial capture between two species of chipmunks. *Evolution*, 69(8):1961–1972, August 2015.

Richard E Green, Johannes Krause, Adrian W Briggs, Tomislav Maricic, Udo Stenzel, Martin Kircher, Nick Patterson, Heng Li, Weiwei Zhai, Markus Hsi-Yang Fritz, Nancy F Hansen, Eric Y Durand, Anna-Sapfo Malaspinas, Jeffrey D Jensen, Tomas Marques-Bonet, Can Alkan, Kay Prüfer, Matthias Meyer, Hernán A Burbano, Jeffrey M Good, Rigo Schultz, Ayinuer Aximu-Petri, Anne Butthof, Barbara Höber, Barbara Höffner, Madlen Siegemund, Antje Weihmann, Chad Nusbaum, Eric S Lander, Carsten Russ, Nathaniel Novod, Jason Affourtit, Michael Egholm, Christine Verna, Pavao Rudan, Dejana Brajkovic, Željko Kucan, Ivan Gušic, Vladimir B Doronichev, Liubov V Golovanova, Carles Lalueza-Fox, Marco de la Rasilla, Javier Fortea, Antonio Rosas, Ralf W Schmitz, Philip L F Johnson, Evan E Eichler, Daniel Falush, Ewan Birney, James C Mullikin, Montgomery Slatkin, Rasmus Nielsen, Janet Kelso, Michael Lachmann, David Reich, and Svante Pääbo. A draft sequence of the neandertal genome. *Science*, 328(5979):710–722, May 2010.

Russell Greenberg and Peter P Marra. *Birds of Two Worlds: The Ecology and Evolution of Migration*. JHU Press, March 2005.

W T Greene. *The amateur's aviary of foreign birds: or, how to keep and breed foreign birds*. L Upcott Gill, London, 1883.

Jared A Grummer, Robert W Bryson, Jr, and Tod W Reeder. Species delimitation using bayes factors: simulations and application to the sceloporus scalaris species group (squamata: Phrynosomatidae). *Syst. Biol.*, 63(2):119–133, March 2014.

Ryan N Gutenkunst, Ryan D Hernandez, Scott H Williamson, and Carlos D Bustamante. Diffusion approximations for demographic inference: DaDi. June 2010.

S Healy and W A Calder. Rufous hummingbird - introduction | birds of north america online. https://birdsna.org/Species-Account/bna/species/rufhum, 2006. Accessed: 2018-8-7.

A J Helbig. Inheritance of migratory direction in a bird species: a cross-breeding experiment with SE-and SW-migrating blackcaps (sylvia atricapilla). *Behavioral Ecology and Sociobiology*, 1991.

Heliconius Genome Consortium. Butterfly genome reveals promiscuous exchange of mimicry adaptations among species. *Nature*, 487(7405):94–98, July 2012.

T D Herbert, J D Schuffert, D Andreasen, L Heusser, M Lyle, A Mix, A C Ravelo, L D Stott, and J C Herguera. Collapse of the california current during glacial maxima linked to climate change on land. *Science*, 293(5527):71–76, July 2001.

Connie A Herr, Paul W Sykes, and John Klicka. Phylogeography of a vanishing north american songbird: the painted bunting (passerina ciris). *Conserv. Genet.*, 12(6):1395–1410, December 2011.

Geoffrey E Hill, Robert R. Sargent, and Martha B. Sargent. Recent change in the winter distribution of rufous hummingbirds. *Auk*, 115(1):240–245, 1998.

Mark A Hixon, F Lynn Carpenter, and David C Paton. Territory area, flower density, and time budgeting in hummingbirds: An experimental and theoretical analysis. *Am. Nat.*, 122(3):366–391, 1983.

Sture Holm. A simple sequentially rejective multiple test procedure. *Scand. Stat. Theory Appl.*, 6 (2):65–70, 1979.

S A Hovan, D K Rea, and N G Pisias. Late pleistocene continental climate and oceanic variability recorded in northwest pacific sediments. *Paleoceanography*, 6(3):349–370, June 1991.

Huateng Huang and L Lacey Knowles. Unforeseen consequences of excluding missing data from next-generation sequences: simulation study of RAD sequences. *Syst. Biol.*, 65(3):357–365, 2014.

Jen-Pan Huang and L Lacey Knowles. The species versus subspecies conundrum: Quantitative delimitation from integrating multiple data types within a single bayesian approach in hercules beetles. *Syst. Biol.*, 65(4):685–699, July 2016.

Birdlife International. BirdLife's online world bird database: the site for bird conservation, 2003.

Darren E Irwin. Sex chromosomes and speciation in birds and other ZW systems. *Mol. Ecol.*, February 2018.

Darren E Irwin, Staffan Bensch, Jessica H Irwin, and Trevor D Price. Speciation by distance in a ring species. *Science*, 307(5708):414–416, January 2005.

Mattias Jakobsson and Noah A Rosenberg. CLUMPP: a cluster matching and permutation program for dealing with label switching and multimodality in analysis of population structure. *Bioinformatics*, 23(14):1801–1806, July 2007.

Ned K Johnson and Carla Cicero. New mitochondrial DNA data affirm the importance of pleistocene speciation in north american birds. *Evolution*, 58(5):1122–1130, May 2004.

Ned K Johnson and Robert M Zink. Genetic evidence for relationships among the Red-Eyed, Yellow-Green, and chivi vireos. *Wilson Bull.*, 97(4):421–435, 1985.

Thibaut Jombart. adegenet: a R package for the multivariate analysis of genetic markers. *Bioinformatics*, 24(11):1403–1405, June 2008.

Thibaut Jombart, Sébastien Devillard, and François Balloux. Discriminant analysis of principal components: a new method for the analysis of genetically structured populations. *BMC Genet.*, 11:94, October 2010.

Zhian N Kamvar, Javier F Tabima, and Niklaus J Grünwald. Poppr: an R package for genetic analysis of populations with clonal, partially clonal, and/or sexual reproduction. *PeerJ*, 2:e281, March 2014.

Andrew D Kern and Matthew W Hahn. The neutral theory in light of natural selection. *Mol. Biol. Evol.*, 35(6):1366–1371, June 2018.

M Kimura. Evolutionary rate at the molecular level. *Nature*, 217(5129):624–626, February 1968.

Brian P Kinlan, Michael H Graham, and Jon M Erlandson. Late-Quaternary changes in the size and shape of the california channel islands: implications for marine subsidies to terrestrial communities. In *Proceedings of the California Islands Symposium*, volume 6, pages 119–130. academia.edu, 2005.

Jeff S Kirby, Alison J Stattersfield, Stuart H M Butchart, Michael I Evans, Richard F A Grimmett, Victoria R Jones, John O'Sullivan, Graham M Tucker, and Ian Newton. Key conservation issues for migratory land- and waterbird species on the world's major flyways. *Bird Conserv. Int.*, 18 (S1):S49–S73, September 2008.

Jonas Korlach, Gregory Gedman, Sarah B Kingan, Chen-Shan Chin, Jason T Howard, Jean-Nicolas Audet, Lindsey Cantin, and Erich D Jarvis. De novo PacBio long-read and phased avian genome assemblies correct and add to reference genes generated with intermediate and short reads. *Gigascience*, 6(10):1–16, October 2017.

Thorfinn Sand Korneliussen, Anders Albrechtsen, and Rasmus Nielsen. ANGSD: Analysis of next generation sequencing data. *BMC Bioinformatics*, 15:356, November 2014.

Vikas Kumar, Fritjof Lammers, Tobias Bidon, Markus Pfenninger, Lydia Kolter, Maria A Nilsson, and Axel Janke. The evolutionary history of bears is characterized by gene flow across species. *Sci. Rep.*, 7:46487, April 2017.

Sangeet Lamichhaney, Jonas Berglund, Markus Sällman Almén, Khurram Maqbool, Manfred Grabherr, Alvaro Martinez-Barrio, Marta Promerová, Carl-Johan Rubin, Chao Wang, Neda Zamani, B Rosemary Grant, Peter R Grant, Matthew T Webster, and Leif Andersson. Evolution of darwin's finches and their beaks revealed by genome sequencing. *Nature*, 518(7539):371–375, February 2015.

Ben Langmead and Steven L Salzberg. Fast gapped-read alignment with bowtie 2. *Nat. Methods*, 9(4):357–359, March 2012.

Adam D Leaché, Matthew K Fujita, Vladimir N Minin, and Remco R Bouckaert. Species delimitation using genome-wide SNP data. *Syst. Biol.*, 63(4):534–542, July 2014.

Adam D Leache, Andreas S Chavez, Leonard N Jones, Jared A Grummer, Andrew D Gottscho, and Charles W Linkem. Phylogenomics of phrynosomatid lizards: conflicting signals from sequence

capture versus restriction site associated DNA sequencing. *Genome Biol. Evol.*, 7(3):706–719, 2015.

Yuyini Licona-Vera and Juan Francisco Ornelas. The conquering of north america: dated phylogenetic and biogeographic inference of migratory behavior in bee hummingbirds. *BMC Evol. Biol.*, 17(1):126, June 2017.

E B Linck and C J Battey. Minor allele frequency thresholds strongly affect population structure inference with genomic datasets. *bioRxiv*, 2017.

Ethan Linck, Eli S Bridge, Jonah M Duckles, Adolfo G Navarro-Sigüenza, and Sievert Rohwer. Assessing migration patterns in passerina ciris using the world's bird collections as an aggregated resource. *PeerJ*, 4:e1871, April 2016.

Stinus Lindgreen. AdapterRemoval: easy cleaning of next-generation sequencing reads. *BMC Res. Notes*, 5:337, July 2012.

Juliette Linossier, Sándor Zsebők, Emmanuelle Baudry, Thierry Aubin, and Hélène Courvoisier. Acoustic but no genetic divergence in migratory and sedentary populations of blackcaps, sylvia atricapilla. *Biol. J. Linn. Soc. Lond.*, 119(1):68–79, September 2016.

Romuald N Lipcius, David B Eggleston, Sebastian J Schreiber, Rochelle D Seitz, Jian Shen, Mac Sisson, William T Stockhausen, and Harry V Wang. Importance of metapopulation connectivity to restocking and restoration of marine species. *Rev. Fish. Sci.*, 16(1-3):101–110, February 2008.

Nicholas A Mason and Scott A Taylor. Differentially expressed genes match bill morphology and plumage despite largely undifferentiated genomes in a H olarctic songbird. *Mol. Ecol.*, 24(12): 3009–3025, 2015.

E Mayr. The bearing of the new systematics on genetical problems; the nature of species. *Adv. Genet.*, 3b(2):205–237, 1948.

Ernst Mayr and Robert J O'Hara. THE BIOGEOGRAPHIC EVIDENCE SUPPORTING THE PLEISTOCENE FOREST REFUGE HYPOTHESIS. *Evolution*, 40(1):55–67, January 1986.

Ernst Mayr and Lester L Short. *Species taxa of North American birds: a contribution to comparative systematics*. [Nuttall Ornithological] Club, 1970.

Eugene M McCarthy. *Handbook of Avian Hybrids of the World*. Oxford University Press, February 2006.

Jimmy A McGuire, Christopher C Witt, J V Remsen, Jr, Ammon Corl, Daniel L Rabosky, Douglas L Altshuler, and Robert Dudley. Molecular phylogenetics and the diversification of hummingbirds. *Curr. Biol.*, 24(8):910–916, April 2014.

Aaron McKenna, Matthew Hanna, Eric Banks, Andrey Sivachenko, Kristian Cibulskis, Andrew Kernytsky, Kiran Garimella, David Altshuler, Stacey Gabriel, Mark Daly, and Mark A DePristo. The genome analysis toolkit: a MapReduce framework for analyzing next-generation DNA sequencing data. *Genome Res.*, 20(9):1297–1303, September 2010.

Colin D Meiklejohn, Kristi L Montooth, and David M Rand. Positive and negative selection on the mitochondrial genome. *Trends Genet.*, 23(6):259–263, June 2007.

Raeann Mettler, H Martin Schaefer, Nikita Chernetsov, Wolfgang Fiedler, Keith A Hobson, Mihaela Ilieva, Elisabeth Imhof, Arild Johnsen, Swen C Renner, Gregor Rolshausen, David Serrano, Tomasz Wesołowski, and Gernot Segelbacher. Contrasting patterns of genetic differentiation among blackcaps (sylvia atricapilla) with divergent migratory orientations in europe. *PLoS One*, 8(11):e81365, November 2013.

Gemma G R Murray, André E R Soares, Ben J Novak, Nathan K Schaefer, James A Cahill, Allan J Baker, John R Demboski, Andrew Doll, Rute R Da Fonseca, Tara L Fulton, M Thomas P Gilbert, Peter D Heintzman, Brandon Letts, George McIntosh, Brendan L O'Connell, Mark Peck, Marie-Lorraine Pipes, Edward S Rice, Kathryn M Santos, A Gregory Sohrweide, Samuel H Vohr, Russell B Corbett-Detig, Richard E Green, and Beth Shapiro. Natural selection shaped the rise and fall of passenger pigeon genomic diversity. *Science*, 358(6365):951–954, November 2017.

Krystyna Nadachowska-Brzyska, Cai Li, Linnea Smeds, Guojie Zhang, and Hans Ellegren. Temporal dynamics of avian populations during pleistocene revealed by Whole-Genome sequences. *Curr. Biol.*, 25(10):1375–1380, May 2015.

Patrik Nosil. Speciation with gene flow could be common. *Mol. Ecol.*, 17(9):2103–2106, May 2008.

Patrik Nosil, Daniel J Funk, and Daniel Ortiz-Barrientos. Divergent selection and heterogeneous genomic divergence. *Mol. Ecol.*, 18(3):375–402, February 2009.

Diana C Outlaw, Gary Voelker, Borja Mila, Derek J Girman, and R Fleischer. EVOLUTION OF LONG-DISTANCE MIGRATION IN AND HISTORICAL BIOGEOGRAPHY OF CATHARUS THRUSHES: A MOLECULAR PHYLOGENETIC APPROACH. *Auk*, 120(2):299–310, April 2003.

Emmanuel Paradis, Julien Claude, and Korbinian Strimmer. APE: Analyses of phylogenetics and evolution in R language. *Bioinformatics*, 20(2):289–290, January 2004.

R A Paynter, Jr. Check-list of birds ofthe world, 1968.

Brant K Peterson, Jesse N Weber, Emily H Kay, Heidi S Fisher, and Hopi E Hoekstra. Double digest RADseq: an inexpensive method for de novo SNP discovery and genotyping in model and non-model species. *PLoS One*, 7(5):e37135, May 2012.

Albert B Phillimore, C David L Orme, Gavin H Thomas, Tim M Blackburn, Peter M Bennett, Kevin J Gaston, and Ian P F Owens. Sympatric speciation in birds is rare: insights from range data and simulations. *Am. Nat.*, 171(5):646–657, May 2008.

Joseph K Pickrell and Jonathan K Pritchard. Inference of population splits and mixtures from genome-wide allele frequency data. *PLoS Genet.*, 8(11):e1002967, November 2012.

J K Pritchard, M Stephens, and P Donnelly. Inference of population structure using multilocus genotype data. *Genetics*, 155(2):945–959, June 2000.

F Pulido, P Berthold, G Mohr, and U Querner. Heritability of the timing of autumn migration in a natural bird population. *Proc. Biol. Sci.*, 268(1470):953–959, May 2001.

Peter Pyle, Steve N G Howell, and Others. *Identification guide to North American birds*. sidalc.net, 1997.

T P Quinn, M J Unwin, and M T Kinnison. Evolution of temporal isolation in the wild: genetic divergence in timing of migration and breeding by introduced chinook salmon populations. *Evolution*, 54(4):1372–1385, August 2000.

A Rambaut, A J Drummond, and M Suchard. Tracer v1. 6 http://beast. bio. ed. ac. uk. *Tracer (visited on 2017-06-12)*, 2014.

Sievert Rohwer. Molt intensity and conservation of a molt migrant (passerina ciris) in northwest mexico. *Condor*, 115(2):421–433, 2013.

Sievert Rohwer and Darren E Irwin. Molt, orientation, and avian speciation. *Auk*, 128(2):419–425, 2011.

Gregor Rolshausen, Gernot Segelbacher, Keith A Hobson, and H Martin Schaefer. Contemporary evolution of reproductive isolation and phenotypic divergence in sympatry along a migratory divide. *Curr. Biol.*, 19(24):2097–2101, December 2009.

Kristen C Ruegg, Eric C Anderson, Kristina L Paxton, Vanessa Apkenas, Sirena Lao, Rodney B Siegel, David F DeSante, Frank Moore, and Thomas B Smith. Mapping migration in a songbird using high-resolution genetic markers. *Mol. Ecol.*, 23(23):5726–5739, 2014.

Stein A Saether, Glenn-Peter Saetre, Thomas Borge, Chris Wiley, Nina Svedin, Gunilla Andersson, Thor Veen, Jon Haavie, Maria R Servedio, Stanislav Bures, Miroslav Král, Mårten B Hjernquist, Lars Gustafsson, Johan Träff, and Anna Qvarnström. Sex chromosome-linked species recognition and evolution of reproductive isolation in flycatchers. *Science*, 318(5847):95–97, October 2007.

J. R. Sauer, D. K. Niven, J. E. Hines, D. J. Jr Ziolkowski, K. L. Pardieck, J. E. Fallon, and W. A Link. The north american breeding bird survey, results and analysis 1966-2015. version 2.07.2017. `https://www.mbr-pwrc.usgs.gov/bbs/`, 2017. Accessed: 2018-5-14.

Molly Schumer, Chenling Xu, Daniel L Powell, Arun Durvasula, Laurits Skov, Chris Holland, John C Blazier, Sriram Sankararaman, Peter Andolfatto, Gil G Rosenthal, and Molly Przeworski. Natural selection interacts with recombination to shape the evolution of hybrid genomes. *Science*, 360 (6389):656–660, May 2018.

J Ryan Shipley, Andrea Contina, Nyambayar Batbayar, Eli S Bridge, A Townsend Peterson, and Jeffrey F Kelly. Niche conservatism and disjunct populations: a case study with painted buntings (passerina ciris). *Auk*, 130(3):476–486, 2013.

Desmond Sieburth and Peter Pyle. Evidence for a prealternate molt-migration in the rufous hummingbird and its implications for the evolution of molts in apodiformes. *Auk*, 135(3):495–505, July 2018.

Theodore R Simons, Frank R Moore, and Sidney A Gauthreaux. Mist netting trans-gulf migrants at coastal stopover sites: the influence of spatial and temporal variability on capture data. *Studies in Avian Biology*, 29:135–143, 2004.

Sonal Singhal, Ellen M Leffler, Keerthi Sannareddy, Isaac Turner, Oliver Venn, Daniel M Hooper, Alva I Strand, Qiye Li, Brian Raney, Christopher N Balakrishnan, Simon C Griffith, Gil McVean, and Molly Przeworski. Stable recombination hotspots in birds. *Science*, 350(6263):928–932, November 2015.

David L Slager, C J Battey, Robert W Bryson, Jr, Gary Voelker, and John Klicka. A multilocus phylogeny of a major new world avian radiation: the vireonidae. *Mol. Phylogenet. Evol.*, 80: 95–104, November 2014.

Linnéa Smeds, Anna Qvarnström, and Hans Ellegren. Direct estimate of the rate of germline mutation in a bird. *Genome Res.*, 26(9):1211–1218, September 2016.

B T Smith, M G Harvey, B C Faircloth, T C Glenn, and others. Target capture and massively parallel sequencing of ultraconserved elements for comparative studies at shallow evolutionary time scales. *Systematic*, 2013.

Brian Tilston Smith, John E McCormack, Andrés M Cuervo, Michael J Hickerson, Alexandre Aleixo, Carlos Daniel Cadena, Jorge Pérez-Emán, Curtis W Burney, Xiaoou Xie, Michael G Harvey, Brant C Faircloth, Travis C Glenn, Elizabeth P Derryberry, Jesse Prejean, Samantha Fields, and Robb T Brumfield. The drivers of tropical speciation. *Nature*, 515(7527):406–409, November 2014.

Alexandros Stamatakis. RAxML version 8: a tool for phylogenetic analysis and post-analysis of large phylogenies. *Bioinformatics*, 30(9):1312–1313, May 2014.

Robert W Storer. Variation in the painted bunting (passerina ciris), with special reference to wintering populations. 1951.

Robert W Storer. Subspecies and the study of geographic variation. *Auk*, 99(3):599–601, 1982.

Brian L Sullivan, Christopher L Wood, Marshall J Iliff, Rick E Bonney, Daniel Fink, and Steve Kelling. ebird: A citizen-based bird observation network in the biological sciences. *Biol. Conserv.*, 142(10):2282–2292, October 2009.

P W Sykes, Jr, S Holzman, and Eduardo E Iñigo-Elias. Current range of the eastern population of painted bunting (passerina ciris). part II: Winter range. *North American Birds*, 61(3):378–406, 2007.

R Core Team and Others. R: A language and environment for statistical computing. 2013.

Jonathan Terhorst, John A Kamm, and Yun S Song. Robust and scalable inference of population history from hundreds of unphased whole genomes. *Nat. Genet.*, 49(2):303–309, February 2017.

Christopher W Thompson. Is the painted bunting actually two species? problems determining species limits between allopatric populations. *Condor*, pages 987–1000, 1991.

David P L Toews, Scott A Taylor, Rachel Vallender, Alan Brelsford, Bronwyn G Butcher, Philipp W Messer, and Irby J Lovette. Plumage genes and little else distinguish the genomes of hybridizing warblers. *Curr. Biol.*, 26(17):2313–2318, September 2016.

US Fish and Wildlife Service and National Marine Fisheries Service. Policy regarding the recognition of distinct vertebrate population segments under the endangered species act. *Fed. Regist.*, 61(26): 4722, 1996.

L J P Vieillot. *Nouv. Dict. Hist. Nat.* D'Abel Lange, Rue de la Harpe, 1817.

G Voelker. Morphological correlates of migratory distance and flight display in the avian genus anthus. *Biol. J. Linn. Soc. Lond.*, 73(4):425–435, August 2001.

Gary Voelker and Jessica E Light. Palaeoclimatic events, dispersal and migratory losses along the Afro-European axis as drivers of biogeographic distribution in sylvia warblers. *BMC Evol. Biol.*, 11:163, June 2011.

Robin S Waples and Oscar Gaggiotti. INVITED REVIEW: What is a population? an empirical evaluation of some genetic methods for identifying the number of gene pools and their degree of connectivity. *Mol. Ecol.*, 15(6):1419–1439, 2006.

Michael S Webster, Peter P Marra, Susan M Haig, Staffan Bensch, and Richard T Holmes. Links between worlds: unraveling migratory connectivity. *Trends Ecol. Evol.*, 17(2):76–83, February 2002.

J T Weir and D Schluter. Calibrating the avian molecular clock. *Mol. Ecol.*, 17(10):2321–2328, May 2008.

Hadley Wickham. *ggplot2: Elegant Graphics for Data Analysis*. Springer, June 2016.

Claus O Wilke. cowplot: streamlined plot theme and plot annotations for 'ggplot2'. *R package version 0. 6*, 2, 2016.

Benjamin M Winger, F Keith Barker, and Richard H Ree. Temperate origins of long-distance seasonal migration in new world songbirds. *Proc. Natl. Acad. Sci. U. S. A.*, 111(33):12115–12120, August 2014.

Shuai Zhan, Wei Zhang, Kristjan Niitepõld, Jeremy Hsu, Juan Fernández Haeger, Myron P Zalucki, Sonia Altizer, Jacobus C de Roode, Steven M Reppert, and Marcus R Kronforst. The genetics of monarch butterfly migration and warning colouration. *Nature*, 514(7522):317–321, October 2014.

Robert M Zink, Ann E Kessen, Theresa V Line, and Rachelle C Blackwell-Rago. COMPARATIVE PHYLOGEOGRAPHY OF SOME ARIDLAND BIRD SPECIES. *Condor*, 103(1):1–10, February 2001.